Exploring host-immune-microbial interactions during intestinal schistosomiasis

Costain, A.H.

CHAPTER 4

Tissue damage and microbiota modifications provoke intestinal type 2 immunity during *Schistosoma mansoni* infection

Alice H. Costain, Alba Cortés, Stefano A. P. Colombo, Arifa Ozir-Fazalalikhan, Emma L. Houlder, Melissa Lawson, Frank Otto, Gordana Panic, Amanda Ridley, Irene Nambuya, Jaqueline J. Janse, Claudia J. de Dood, Meta Roestenberg, Angela van Diepen, Cornelis H Hokke, Jonathan R. Swann, Gabriel Rinaldi, Cinzia Cantacessi, Andrew S. MacDonald, Hermelijn H. Smits

Manuscript in preparation

Tissue damage and microbiota modifications provoke intestinal type 2 immunity during Schistosoma mansoni infection

AUTHOR INFORMATION

Alice H. Costain[1,2], Alba Cortés[3,4], Stefano A. P. Colombo[2], Arifa Ozir-Fazalalikhan[1], Emma L. Houlder[2], Melissa A.E. Lawson[2], Frank Otto[1], Gordana Panic[5], Amanda Ridley[2], Irene Nambuya[2], Jaqueline Janse[1], Claudia J. de Dood[1], Meta Roestenberg[1], Angela van Diepen[1], Cornelis H Hokke[1], Jonathan R. Swann[5], Gabriel Rinaldi[6], Cinzia Cantacessi[3], Andrew S. MacDonald[2]*, Hermelijn H. Smits[1]*

1. Department of Parasitology, Leiden University Medical Center, Leiden, Netherlands
2. Lydia Becker Institute of Immunology and Inflammation, Faculty of Biology, Medicine and Health, University of Manchester, UK
3. Department of Veterinary Medicine, University of Cambridge, UK
4. Departament de Farmàcia i Tecnologia Farmacèutica i Parasitologia, Facultat de Farmàcia, Universitat de València, Spain
5. School of Human Development and Health, University of Southampton
6. Wellcome Sanger Institute, Wellcome Genome Campus, Hinxton, CB101SA, UK

*Co-corresponding authors: Andrew S. MacDonald (andrew.macdonald@manchester.ac.uk) and Hermelijn Smits (h.h.smits@lumc.nl)

ABSTRACT

During mammalian infection with *Schistosoma mansoni*, parasite eggs pierce the intestinal wall as they cross into the lumen. Despite this destructive process being central to schistosome-associated pathology, there are limited studies addressing the impact of egg transit on intestinal barrier integrity, microbiota composition, and host immune responses. Here, we present a detailed characterisation of the intestinal environment during murine schistosomiasis, using a combination of high vs low dose, and mixed sex (egg production) vs male worm only (no egg production) infections. We show that intestinal barrier function was compromised during patent (egg producing) infections, with evidence for increased intestinal permeability and systemic responses to gut bacteria. Infection intensity altered the kinetics of these barrier changes. Patent infections induced Type 2 dominated immune responses in the mesenteric lymph nodes and colonic lamina propria, as characterised by eosinophilia, elevated Th2 cell cytokine and transcription factor expression, and increased Type 2 associated factors (Relmα and Ym1) in host faeces. Importantly, this dramatic Type 2 shift coincided with significant alterations to the intestinal microbiota that became more marked as infection progressed, and with increased infection intensity. Finally, using germ free mice and faecal transplants, we found that the schistosome-associated microbiota induce a Type 2 profile in recipients. Our data elevates mechanistic understanding of schistosome-mediated immune modulation and provides evidence for a novel tripartite interaction between host, schistosome and commensal bacteria in development of the intestinal immune response during infection.

Keywords

Schistosoma, microbiota, Th2, intestinal permeability

Abbreviations

Ag, Antigen; CAA, circulating anodic antigen; DC, Dendritic cell; FITC-dextran, Fluorescein isothiocyanate–Carboxymethyl–Dextran; GF, Germ-free; IL-, Interleukin; LP; Lamina Propria; MLN; mesenteric lymph node; pDC, Plasmacytoid dendritic cell; SEA, Soluble egg antigen; SIC, small intestinal content; SPF, specific pathogen free; Th, T Helper; TMA, Trimethylamine; TMAO, Trimethylamine oxide; Treg, Regulatory T cell; WPI, weeks post infection.

INTRODUCTION

Schistosomiasis is a neglected yet significant tropical disease, spread by exposure to infectious *Schistosoma* larvae (cercariae) found in infested water in endemic regions. An estimated 250 million individuals have overt disease[1], with *S. haematobium*, *S. mansoni* and *S. japonicum* being the three main causative species. The disease that develops is indicative of where mature adult worms live and deposit their eggs within the host. During *S. mansoni* and *S. japonicum* infections, adult worms reside and lay eggs within the mesenteric vessels, with these eggs either piercing through intestinal tissue and escaping the host or being swept by portal blood flow to trap them within the liver. Tissue transiting or entrapped eggs become the focal points of T helper 2 (Th2) dominated, granulomatous inflammation. These inflammatory reactions serve as protective shields that destroy eggs and, enigmatically, facilitate their movement into the intestinal lumen[2]. If the host immune reaction ineffectively or overzealously deals with persistent egg-driven Th2 inflammation, severe obstructive and potentially life-threatening disease may result[3–5].

Schistosoma parasites are adept regulators of the host immune system, crafting an immunological environment that promotes their long-term survival whilst minimising bystander tissue damage within their host[6]. Schistosome modification of host immunity is in part achieved through the active secretion of immunomodulatory molecules[7–9], each mediating their effects through distinct pathways, cell types and at different stages of infection[10]. In addition to parasite products, host immune responses are instructed by stress signals, endogenous molecules released upon tissue damage[11], and environmental stimuli such as the microbiota[12,13].

The mammalian microbiota has a profound impact on the calibration of host immunity, with almost every disease and tissue system reporting sensitivity to microbiota composition[14]. In schistosomiasis, qualitative and quantitative changes in intestinal microbiota composition have been reported across experimental and natural infections[15–18], with accompanying pathology and immune reactions showing sensitivity to shifts in bacterial community structure[16,17,19,20]. It remains unclear whether schistosomes actively modify the composition of the microbiota in support of their infectious lifecycle, or whether the perturbed microbiota is a consequence of egg-driven tissue destruction and/or pronounced Type 2 immunity.

In this study, we investigated the extent of intestinal inflammation caused by schistosome egg transit during infection and explored the impact this process has on the intestinal microbiota, as well as how that microbiota influences host immunity. Our results revealed the dramatic impact

schistosome eggs have on the intestinal environment, including a reduction in intestinal barrier function, skewed immune profiles, and strikingly altered microbiota composition. Then, through faecal transplant studies we have identified a critical role for the intestinal microbiota in dictating host intestinal Type 2/17 immune responses. Combined, our data suggests a novel, microbial-based mechanism by which parasitic worms skew host immunity.

MATERIALS AND METHODS

Animals and Ethics statement

Age matched, female C57BL/6 mice (Envigo) were housed under specific pathogen free (SPF) conditions at Leiden University Medical Centre (The Netherlands) or the University of Manchester (UK). For germ-free (GF) experiments, GF mice were bred in isolators at the University of Manchester Gnotobiotic Facility and maintained in GF isolators or individually ventilated cages for experiment duration. For recolonisation experiments, GF mice were colonised by a single oral gavage of faeces isolated from either uninfected or schistosome infected mice. Mice were culled 2 or 3 weeks post gavage and maintained under GF conditions for this duration. Experiments based in the Netherlands were performed in accordance with the guidelines and protocols approved by the Ethics Committee for Animal Experimentation of the University of Leiden. UK experiments were performed under a project license granted by the Home Office UK and performed in accordance with the United Kingdom Animals (Scientific Procedures) Act of 1986.

Schistosome infection

Biomphalaria glabrata snails infected with a Puerto Rican strain of *S. mansoni* were maintained at Leiden University Medical Centre or obtained from K. Hoffman (Aberystwyth University, UK). Mice were percutaneously infected with male and female *S. mansoni* cercariae (mixed-sex infection) or male cercariae only (single-sex infection). Infections were performed at doses of 40 cercariae (low dose infection) or 180 cercariae (high dose infection). Cercariae sex was determined by purpose-made multiplex PCR, targeting schistosome sex-specific sequences, as described previously[21]. At the time of euthanasia, infection was confirmed in single-sex and mixed-sex infected mice by the detection of the regurgitated worm product, Circulating Anodic Antigen (CAA) in mouse serum[22]. At time points following egg deposition (week 7 onwards), mixed-sex infections were further confirmed by macroscopic evaluation of the liver and intestine, followed by whole intestine digestion in 4% KOH (24hr, 37°c) for egg counts. Mixed-sex infected mice with no visible sign of infection were excluded from analysis. A separate cohort of mice were evaluated at each specified timepoint.

FITC dextran intestinal permeability assay

Intestinal permeability was assessed *in vivo* by administration of the fluorescent tracer, fluorescein isothiocyanate-conjugated (FITC) dextran (4kDa) at dose of 0.6mg/g BW (Sigma Aldrich). Mice were fasted for 4h prior to the oral administration of FITC-dextran. 2h later, ~100µl of blood was collected by tail vein bleed, placed into heparinised tubes, and centrifuged (500xg, 10 minutes, RT) to collect plasma. FITC concentration was analysed using fluorimetry at excitation and emission wavelengths of 485nm and 525nm respectively. For standard curve creation, FITC-dextran was serially diluted in plasma obtained from non-infected control mice. Permeability testing was conducted one week prior to mice being culled for further sampling.

Cell isolation

Single cell suspensions were prepared from the mesenteric lymph nodes (MLNs), colonic lamina propria (LP) and spleen. Leukocytes were isolated from colonic LP as previously described[23,24], with some modifications to account for the high toxicity associated with schistosome infections. Colons were removed by cutting below the caecum, with care taken to remove as much fat as possible from the colon exterior. Using blunt tip scissors, colons were opened longitudinally and washed vigorously in ice-cold PBS (Sigma). In studies involving microbiome analysis, intestines were removed using sterile scissors, and a sterile razor blade was used to squeeze out any luminal content, which was transferred directly into sterile tubes, snap frozen and stored at -80 °C. After removal of luminal content, intestines were chopped into smaller segments (1-2cm) and placed in ice-cold RPMI 1640 (Sigma) containing 3% fetal bovine serum (FBS), 20 mM HEPES (Sigma) and 2mM EDTA (Sigma). After vigorous vortexing for 10 seconds, colon segments were washed with pre-warmed PBS, and the epithelial fraction removed by incubation in prewarmed RPMI 1640 containing 3% FBS, 20 mM HEPES, 5mM EDTA, and 0.5 mM freshly thawed dithiothreitol (DTT; Life Technologies) for 10 minutes at 37°C with shaking at 200rpm. Samples were vortexed, media was drained and replaced for an additional 10 minute incubation. The remaining tissue (LP and muscularis) was digested at 37°C for 30 minutes with continuous stirring (450rpm) in pre-heated RPMI 140 containing 10% FBS, 20 mM HEPES, 2 mM L-glutamine (Sigma), 1x non-essential amino acids (Sigma)**,** 1mM sodium pyruvate (Sigma), 0.5mg/ml Liberase TL (Roche), and 0.25 mg/ml DNase I type VI (Sigma). Digestion was quenched by placing on ice and topping up with ice cold media containing 10% FBS. Samples was sequentially passed through a 70µm and 40-µm cell strainer, and after pelleting, resuspended in 10% FBS containing media. MLNs were carefully removed from the exterior of the small intestine and mesenteries respectively, before 30 minute incubation with

0.15mg/ml Liberase TL and 0.05µg/ml DNase I type VI in HBSS at 37°C in a shaking incubator. Digested tissue was subsequentially passed through a 40-µm cell strainer, and after pelleting, were resuspended in 10% FBS supplemented media. Spleens were processed in a similar manner to the MLNs, with the inclusion of an additional RBC lysis step after cell straining. Single-cell suspensions were counted using haemocytometers and re-suspended in X-VIVO™ Serum-free media (Lonza), before taken further for flow cytometry or PMA/ionomycin stimulation.

Flow cytometry

Equal numbers of cells were stained per sample, washed with PBS and stained with live/dead fixable aqua dead cell stain kit (1:400; Thermo Scientific) or Zombie UV dye (1:2000, BioLegend) for 10 minutes at room temperature. Samples were subsequently blocked with 5 µg ml^{-1} FcγR-binding inhibitor (2.4G2; Biolegend) in FACS buffer (PBS containing 2% FBS and 2mM EDTA), before staining with relevant antibodies at 4 °C for 30 minutes (Table 1). For detection of intracellular markers, cells were further fixed and permeabilized with BD Cytofix/Cytoperm™ for 1h at 4°C, then stained for specified intracellular markers. Cell surface markers and intracellular cytokines were stained using combinations of fluorescently labelled primary or secondary antibodies. For intracellular cytokine staining, cells were plated at 0.4-1 × 10^6/well in volumes of 100µl and stimulated for 3h in the presence of 30ng/ml PMA, 1 µg/ml Ionomycin and 1 µg/ml Golg Stop (BD). Cells were further processed for flow cytometry as described above.

Company	Target	Clone		Company	Target	Clone
Invitrogen	CD3	17A2		Invitrogen	CD11b	M1/70
Biolegend	CD4	RM4-5		Invitrogen	CD11c	N418
Biolegend	CD8	53-6.7		BD	CD19	Ebio(ID3)
Biolegend	CD25	PC61		Biolegend	CD64	x54-5/7.1
Ebioscience	CD44	Im7		Biolegend	F4/80	BM8
Biolegend	CD62L	MeL-14		Biolegend	Ly6C	HK1.4
Biolegend	IFN-y	XMG1.2		Biolegend	MHC-II	M5/114.15.2
Biolegend	IL-10	JES5-16E3		Biolegend	PDCA-1	927
Ebioscience	IL-13	ebio13A		BD	Siglec-F	E50-2440
Biolegend	IL-17	TC11-1810.1		Ebioscience	Ter-119	TER-119
Biolegend	IL-4	11B11		Biolegend	XCR1	ZET
Ebioscience	IL-5	TRFK.5		Ebioscience	Gata-3	TWAJ
Invitrogen	TCRb	H57-597		Biolegend	GITR	DTA-1
Invitrogen	Foxp3	FJK-16s		Ebioscience	RORyt	B2D
Biolegend	CD45	30-f11		Biolegend	T-bet	4Bio

Table 1. List of Flow cytometry antibodies and their clones

DNA Isolation and Microbial 16S rRNA Gene Sequencing

Genomic DNA was isolated from faecal samples collected directly form the colon of mice infected with either mixed- or single-sex *S. mansoni* at several weeks post-infection (i.e., 4, 7, 12 and 14 weeks) and naïve counterparts using a PowerSoil DNA Isolation Kit (Qiagen) according to manufacturers' instructions. Parallel to the samples, two non-template negative controls were subjected to the DNA isolation protocol and downstream analysis to ensure no undesired contamination occurred. High-throughput sequencing of the prokaryotic 16S rRNA gene was performed on an Illumina MiSeq platform[25]. Briefly, the V3-V4 region was PCR-amplified using universal primers[26] that contained the Illumina adapter overhang nucleotide sequences, 5 ng/µl of template DNA, and the Q5® NEBNext hot start high-fidelity DNA polymerase (New England Biolabs) with thermocycling as follows: 2 minutesat 98 °C, 20 cycles of 15 s at 98 °C – 30 s at 63 °C – 30 s at 72 °C, and a final elongation step of 5 minutes at 72 °C. Resulting amplicons were purified using AMPure XP beads (Beckman Coulter) and set up for the index PCR using Nextera XT index primers (Illumina), Q5® NEBNext hot start high-fidelity DNA polymerase, and the following thermocycling protocol: 3 minutes at 95 °C, 8 cycles of 30 s at 95 °C – 30 s at 55 °C – 30 s at 72 °C, and 5 minutes at 72 °C. Indexed samples were purified using AMPure XP beads, quantified using the Qubit dsDNA high sensitivity kit (Life Technologies), and equal amounts from each sample were pooled. The resulting pooled library was quantified by real-time PCR using the NEBNext library quantification kit (New England Biolabs) and sequenced using the v3 chemistry (2x300 bp paired-end reads, Illumina).

Paired-end demultiplexed Illumina reads were processed using the Quantitative Insights Into Microbial Ecology (QIIME2; 2019.1 release) software suite[27] .Sequences were then quality filtered, dereplicated, chimeras identified, and paired-end reads merged in QIIME2 using DADA2[28]with default settings. A phylogenetic tree was generated using the align-to-tree-mafft-fasttree pipeline in the q2-phylogeny plugin. Bray-Curtis dissimilarity between samples was calculated using core-metrics-phylogenetic method from the q2-diversity plugin. Classification of Operational Taxonomic Units (OTUs) was performed using a Naïve Bayes algorithm trained using sequences representing the bacterial V3-V4 rRNA region available from the SILVA database (https://www.arb-silva.de/download/archive/qiime; Silva_132)[29] (Quast et al., 2013), and the corresponding taxonomic classifications were obtained using the q2-feature-classifier plugin in QIIME2. The classifier was then used to assign taxonomic information to representative sequences of each OTU.

Statistical analyses were performed using the online software Calypso (cgenome.net/calypso/)[30]. For data normalisation, cumulative-sum scaling (CSS) was applied to the OTU table, followed by log2 transformation (CSS+log) to account for the non-normal distribution of taxonomic counts data. Samples were ordinated using unsupervised Principle Coordinates Analysis (PCoA) based on Bray-Curtis dissimilarities, or Non-metric multidimensional scaling (NMDS). Supervised Canonical Correspondence Analysis (CCA) was performed on samples collected at individual time points and setting the type of infection as explanatory variable. Following rarefaction of raw data, differences in microbial alpha diversity (Shannon diversity), richness and evenness were evaluated using ANOVA. Where genera were ranked by abundance this was achieved by calculating the mean of the total normalized readcounts per genera across all samples. Heatmaps were generated using pheatmap (version 1.0.12). All other graphs were produced using ggplot2 (version 3.3.3).

Metabolomics

Small intestinal content (SIC) samples were randomised and 20-50 mg of sample weighed out into a 2 ml sterile screw-top tube. 10-20 zirconium beads were proportionally added, as well as $_{d}H2O$ at a 2:7 weight to water ratio. The contents were homogenized (6,500 rpm, 2 cycles of 45 seconds), then centrifuged at 13,000 x g for 20 minutes. Subsequently, 54 µl of the supernatant was transferred to an Eppendorf tube and 6 µl of phosphate buffer solution (1.5 M KH2PO4, 2 mM NaN3, 1 % TSP, pH 7.4) was added and the contents vortexed. 50 µl of the mixture was added to 1.7 mM tubes. A quality control sample was generated by pooling from each sample and combining with buffer as described above.

One dimensional 1H NMR spectra were acquired on a Bruker Advance III HD 600 MHz NMR spectrometer (Bruker Biospin GmbH, Rheinstetten, Germany), equipped with a SampleJet system and a cooling rack of refrigerated tubes at 6° C. For serum samples, a relaxation edited spin-echo using the 1D-Carr-Purcell-Meiboom-Gill (CPMG) presat pulse sequence was applied to all samples, analysed at a temperature of 300 K. For SIC samples, a standard one-dimensional solvent suppression pulse sequence was used (relaxation delay, 90° pulse, 4 µs delay, 90° pulse, mixing time, 90° pulse, acquire FID), analysed at a temperature of 310 K. For each sample, 128 transients were collected in 64K frequency domain points with a spectral window set to 20 ppm.

Automated processing of the spectra was performed using TopSpin 3.6 (Bruker Corporation, Germany) including spectral calibration, phase and baseline correction. The resulting raw NMR spectra were imported into MATLAB (Version 2018a, Mathworks Inc). After digitization of the

spectra, redundant peaks (TSP, H2O) were removed. The spectra were manually aligned to quality control samples and reference peaks using Recursive Segment-Wise Peak Alignment 1 (University of Southampton). Metabolite identification was performed using an in-house metabolite library, cross-referencing with the Human Metabolome Database (https://hmdb.ca/) and Statistical Total Correlation Spectroscopy (STOCSY) 3. The relative concentrations of all age associated metabolites were calculated from the spectral data using trapezoidal numerical integration.

Faecal ELISAs and occult blood detection

Faecal pellets were reconstituted in PBS containing 0.1% Tween 20 (100mg/ml) and vortexed thoroughly to attain a homogenous faecal suspension. Samples were centrifuged (10 minutes, 4°C, 12,000 rpm) to collect a supernatant that was stored at -20°C until later analysis. Faecal levels of lipocalin (Lcn-2; R&D Systems), Ym1 and RELMα (both PeproTech) were analysed by ELISA as per manufacturer's instructions. Faecal blood was detected using Hemdetect occult blood detection kits (Dipro).

Cytokine and serum Ab analysis

Serum levels of Ym1, RELMα (both Peprotech) and IgE (BD**)** were measured using paired capture and detection antibodies, with quantity assessed via standard curve. Levels of IFNγ, IL-5, IL-12 and TNFα were measured by Cytometric Bead Array (CBA) according to manufacturer's instructions (BD). Commensal bacteria-specific ELISAs were conducted as previously described[31]. Briefly, caecal content from a naïve C57BL/6 SPF mouse was homogenised and centrifuged at 1,000 rpm to remove large aggregates. The resulting supernatant was washed twice with sterile PBS by centrifugation for 1 minute at 8,000 rpm. For the final wash, the bacterial pellets were re-suspended in 2 ml ice-cold PBS and sonicated on ice. Samples were subsequently centrifuged at 20,000xg for 10 minutes, and supernatants recovered for a crude commensal bacterial Ag preparation. To measure levels of commensal bacteria specific Total IgG, 96 well plates (NUNC Maxisorp) were coated with 5µg/mL of commensal bacterial Ag and sera were incubated at dilutions of 1:50. Alkaline phosphatase–conjugated goat anti–mouse IgG (SouthernBiotech) was added to plates (1:1000), followed by liquid PNPP substrate, with absorbances read at 405nm. For the presence of IgG1 and IgG2c reactive against SEA, 96 well plates were coated with 5 µg/mL and serum was added at dilutions of 1:1000. SEA-specific isotypes were detected using alkaline phosphatase–conjugated goat anti–mouse IgG1 or IgG2c antibodies (Southern Biotech). Absorbance at 405 was determined as above. For all ELISAs, blocking steps were conducted with 1% bovine serum albumin (BSA, Sigma) for 1h at room

temperature. After blocking and between individual incubation steps, plates were washed 3 times with PBS containing 0.05% Tween (Sigma).

RNA extraction and quantitative PCR analysis

RNA from snap-frozen MLNs or ileum was extracted using TriPure isolation reagent (Roche) and translated to cDNA using SuperScript™ III Reverse Transcriptase and Oligo (dT; Life Technologies). Quantitative PCR was performed with SYBR Green Master Mix (Applied Biosystems) using a Biorad CFX96 Real-time system C1000 thermal cycle. Expression levels were normalized to housekeeping gene Ribosomal Protein Lateral Stalk Subunit P0 (RPLP0). The primers used are given in the table below.

Target gene	Forward primer	Reverse primer
Cdh1	CCAAGCACGTATCAGGGTCA	ACTGCTGGTCAGGATCGTTG
Chi3l3	ACAATTAGTACTGGCCCACCAGGAA	TCCTTGAGCCACTGAGCCTTCA
Cldn2	ATCACCACAGCTTGTGACCC	TCTAGAAAACGGAGCCGTCC
Cldn3	CCTAGGAACTGTCCAAGCCG	CCCGTTTCATGGTTTGCCTG
Gapdh	TGTGTCCGTCGTGGATCTGA	CCTGCTTCACCACCTTCTTGAT
Ifng	CGGCACAGTCATTGAAAGCC	TGTCACCATCCTTTTGCCAGT
Il10	GACAACATACTGCTAACCGACTC	ATCACTCTTCACCTGCTCCACT
Il12a	GGTGAAGACGGCCAGAGAAA	GTAGCCAGGCAACTCTCGTT
Il13	CCCTGGATTCCCTGACCAAC	GGAGGCTGGAGACCGTAGT
Il17a	TCATCCCTCAAAGCTCAGCG	TTCATTGCGGTGGAGAGTCC
Il33	CTGCAAGTCAATCAGGCGAC	ACGTCACCCCTTTGAAGCTC
Il4	CCTCACAGCAACGAAGAACA	ATCGAAAAGCCCGAAAGAGT
Il5	TGGGGGTACTGTGGAAATGC	CCACACTTCTCTTTTTGGCGG
Lcn2	GCCACTCCATCTTTCCTGTTG	AAGAGGCTCCAGATGCTCCTT
Nod2	CTGTCCAACAATGGCATCACC	GTTCCCTCGAAGCCAAACCT
Nos2	TCCTGGACATTACGACCCCT	CTCTGAGGGCTGACACAAGG
Ocln	GTCCTCCTGGCTCAGTTGAA	AGATAAGCGAACCTTGGCGG
Rn18s	GACTCAACACGGGAAACCTC	AGACAAATCGCTCCACCAAC
Rplp0	TCTGGAGGGTGTCCGCAACG	GCCAGGACGCGCTTGTACCC
Tnf	GTCCCCAAAGGGATGAGAAG	CACTTGGTGGTTTGCTACGA
Tjp	GGAGATGTTTATGCGGACGG	CCATTGCTGTGCTCTTAGCG

Table 2. Primers for qPCR

Statistics

Statistical analysis of 16S rRNA Gene Sequencing was performed as described. All other statistics were performed using GraphPad Prism 9 software. Data are shown as mean values ± S.E.M. Where applicable, experimental groups were analysed by unpaired t-test, one-way or two-way analysis of variance (ANOVA) followed by Tukey's post-test as appropriate. Significant differences were defined at $P < 0.05$.

RESULTS

Increased intestinal barrier permeability during chronic egg producing *S. mansoni* infections

During active *S. mansoni* infections, eggs continuously transit from the mesenteric vasculature across the intestinal wall for eventual release into the environment via the faeces[32]. With several hundred eggs produced per day per worm pair[33], this process causes significant damage to the intestinal wall[6]. To investigate whether egg transit reduces mucosal barrier function, we assessed intestinal leakage and inflammation at several key stages of the *S. mansoni* lifecycle: pre-patent acute (week 3), the start of post-patent acute (week 6), the midst of post-patent acute disease (week 8) and chronic stages of disease (weeks 11 and 13) (Figure 1A). In addition, to distinguish the influence of worm or egg-derived signals on intestinal function, comparison was made between mice infected with patent, dual-sex schistosome infections (mixed-sex infection), or mice infected with male schistosomes only (single-sex infection), in which no eggs are produced[21]. Measurement of serum circulating anodic antigen (CAA)[34] levels confirmed similar infection burdens between the single- and mixed-sex infection groups (Supplementary Figure 1A).

Intestinal permeability, as evaluated via oral administration of FITC labelled dextran (Figure 1C), showed that until 8 weeks post infection, no measurable differences in FITC-dextran levels were detected in the plasma of mixed-sex, single-sex or uninfected control mice. However, from week 11 of infection onwards, intestinal permeability was significantly higher in mixed-sex infected mice in comparison to single-sex infected or uninfected controls. These permeability changes did not correlate with individual mouse infection intensity, as measured by intestinal egg burden (Figure 1B) or levels of the regurgitated worm Ag, CAA (Supplementary Figure 1A).

To test whether, as a consequence of increased gut barrier permeability, luminal content (including intestinal bacteria and their products) may have permeated local tissues or systemic circulation, serum levels of commensal bacteria-specific IgG were measured across the course of infection (Figure 1D). In keeping with observed permeability kinetics (Figure 1C), significantly higher levels of

commensal bacteria-specific IgG were detected in the serum of mixed-sex infected mice at weeks 12 and 14 post infection, but not in naïve or single-sex infected mice (Figure 1D). Similarly, faecal occult blood was detected in faeces from mixed-sex infection at weeks 8, 12 and 14, at respective percentages of 12.5%, 87.7% and 75% (Figure 1F&G). In addition to occult blood, faecal pellets were analysed for levels of lipocalin (LCN-2), an anti-microbial peptide that can be found within neutrophilic granules or readily released from the intestinal epithelium upon damage[35]. Faecal lipocalin levels were significantly higher in mixed-sex infected mice from week 8 onwards (Figure 1E). Despite identifying multiple signs of disrupted intestinal barrier integrity during chronic disease, we observed no differences in mRNA expression of intestinal tight junction molecules such as claudin-2, claudin-3, occludin, E-cadherin and tight junction protein (TJP) (Supplementary Figure 1B).

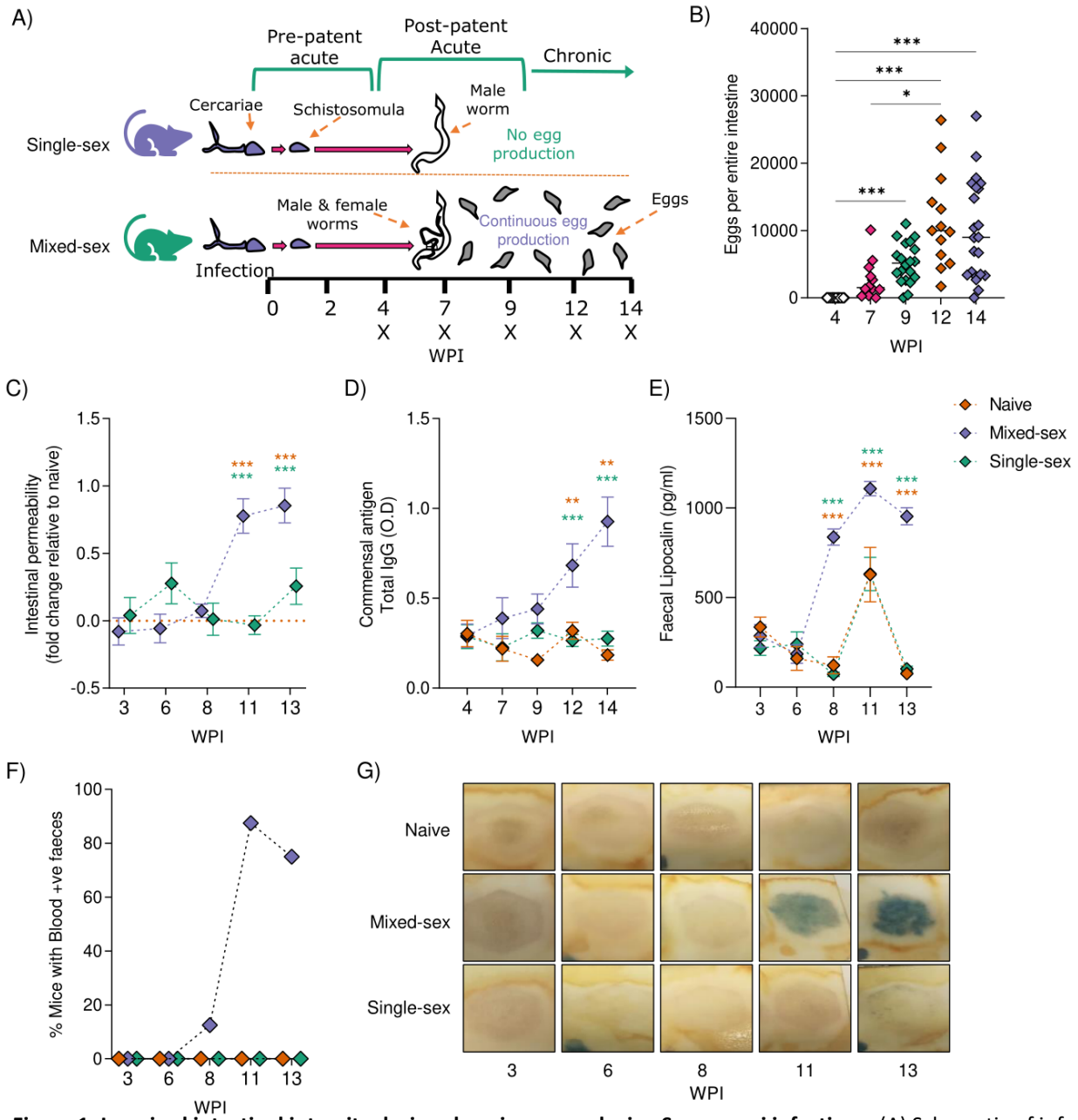

Figure 1. Impaired intestinal integrity during chronic egg producing S. mansoni infections. (A) Schematic of infection setup (WPI, weeks post infection). C57BL/5 mice were infected with ~40 S. mansoni cercariae, of either male and female gender (mixed-sex infection), or male only (single sex infection). Infections lasted 4, 6, 9, 12 or 14 weeks (indicated by X) and permeability was measured 1 week prior by FITC-dextran oral gavages. (B) Intestinal egg counts in mixed-sex infected mice at indicated time points. (C) Changes in intestinal permeability over the course of infections as measured by the detection of FITC-dextran (ELISA) in serum of mice 2 hours after oral gavage. Data presented as fold change relative to naïve controls. (D) Relative serum IgG specific to commensal bacteria throughout time-course. (E) Faecal Lipocalin, a marker of intestinal epithelial damage, was measured in the faeces of mice on the same weeks of FITC dextran permeability measurement. (F) Percentage of mice positive for blood in faeces. (G) Images depicting occult blood detection (blue) in faecal samples of indicated mice groups. Data presented as mean +/- SEM. n=12-24 mice per group pooled across two (D-G) or three separate experiments (B&C). Significant differences are indicated by * $p < 0.05$, ** $p < 0.01$, *** $p < 0.001$ and calculated by one-way ANOVA (B) or two-way ANOVA (C-E). Significant differences between naïve vs mixed-sex infected mice, and single-sex vs mixed-sex infected mice are indicted by orange (*) and green asterisks (*) respectively. Significant differences between naïve and single-sex infected mice are indicated by #. n= 18-24 mice per group from 3 pooled experiments.

Pronounced intestinal Th2 inflammation in patent mixed-sex infections only

After identifying distinct differences in intestinal integrity between patent and non-patent infections, we next addressed the influence of egg migration on local immune responses. We first evaluated the kinetics of mRNA expression of cytokines within the MLNs of mixed-sex and single-sex infected mice across the course of infection, and naïve controls (Figure 2 A&B). In support of existing literature on systemic responses[36,37], mixed-sex infections were accompanied by pronounced Th2 polarisation in terms of *il4*, *il5* and *il13* expression, from week 9 onwards (Figure 2A). After peaking at 9 or 12 weeks post infection, Th2 cytokine expression declined, but remained elevated in comparison to pre-patency. In contrast to mixed-sex infected mice, the expression of Th2-associated cytokines in single-sex infections remained comparable to naïve irrespective of time-point. Regarding Th1 associated cytokines, *ifng*, *il12* and *tnfa* mRNA expression remained similar between all groups at weeks 4-9 (Figure 2B). However, by week 14 we observed a modest but significantly increased Th1 cytokine expression profile in both mixed- and single-sex infection groups (Figure 2B). These MLN gene expression patterns were reflected at a systemic level (Supplementary Figure 2), with only mixed-sex infections showing elevated serum levels of Th2 associated mediators IL-5, RELMα, Ym1 (Supplementary Figure 2A), total IgE and SEA-specific IgG1 (Supplementary Figure 2C). From a Th1 perspective, we observed significantly higher serum levels of IFNγ, IL-12, TNF-α (Supplementary Figure 2B), and SEA-specific IgG2c (Supplementary Figure 2C), in single-sex infected mice at chronic disease stages.

Next, reasoning that mediators produced locally due to egg induced tissue damage may leak into the intestinal lumen, faecal pellets were analysed for various inflammatory mediators and cytokines (Figure 2C). Interestingly, while many cytokines showed no difference between the experimental groups (IL-6, IL-1β, and IFN-β; data not shown) or could not be detected (IL-13, IL-4, IL-10; data not shown), faeces from mixed-sex infected mice showed significantly higher levels of Type 2 mediators, Ym1 and RELMα from week 8 of infection onwards.

Focussing on week 14, a time point at which egg migration has long been established and permeability is pronounced (Figure 1), we observed similar trends for MLN $CD4^+$ T cell cytokine production (Figure 2D&E) and ileal mRNA expression (Figure 2F). Notably, the production and expression of Th2 associated cytokines was elevated in mixed-sex infected mice only, with the exception of IL-5, whose secretion from $CD4^+$ T cells was comparable in single-sex infected mice. Moreover, despite the damage caused by egg transit, patent infection did not significantly influence levels of MLN cell expression or production of inflammatory IFNγ or counter regulatory IL-10.

Additionally, ileal tissue from mixed-sex infected mice expressed similar mRNA expression profiles of Th2 and Th1 cytokines to MLN (Figure 2F), as well as elevated expression of genes associated with alternative activation of macrophages (*arg1* and *chil3*), and the damage associated alarmin *il25* (Figure 2G). No differences were observed in the expression of *nos2*, which is linked to classical macrophage activation[38].

Figure 2. Pronounced Th2 orientated immune profiles in mixed-sex infections. (A&B) The mRNA expression of Th2 (IL-4,5 &13) and Th1 (IL-12,TNF & IFN-y) cytokines in the mesenteric lymph nodes (MLNs) of naïve, mixed-sex and single-sex infected mice (both infected with 40 cercariae) at indicated time-points. Data normalized against HK gene RPLP0 and represented as fold change relative to naïve. (C)) Faecal levels of RELMα and Ym1 (D) Cytokine secretion from PMA ionomycin stimulated MLN cells at week 14 of infection.(E) Representative flow plots for IL-4 secretion, pre-gating on live CD45+ TCRβ+ CD4+ cells. (F&G) The colonic mRNA expression of indicated genes at 14 weeks post infection. Data normalised against HK pool (RPLP0, β2m, β-actin and s18) and represented as fold change relative to nave. Data presented as mean +/- SEM. n=4-7 from one single experiment (F&G) or pooled across two separate experiments (A,B,C,D&E). Significant differences were determined by one-way (D,F&G) or two-way ANOVA (A-C) followed by Tukey post hoc tests. *p < 0.05, **p < 0.01, ***p < 0.001. Significant differences between naïve vs mixed-sex infected mice, and single-sex vs mixed-sex infected mice are indicted by orange (*) and green asterisks (*) respectively.

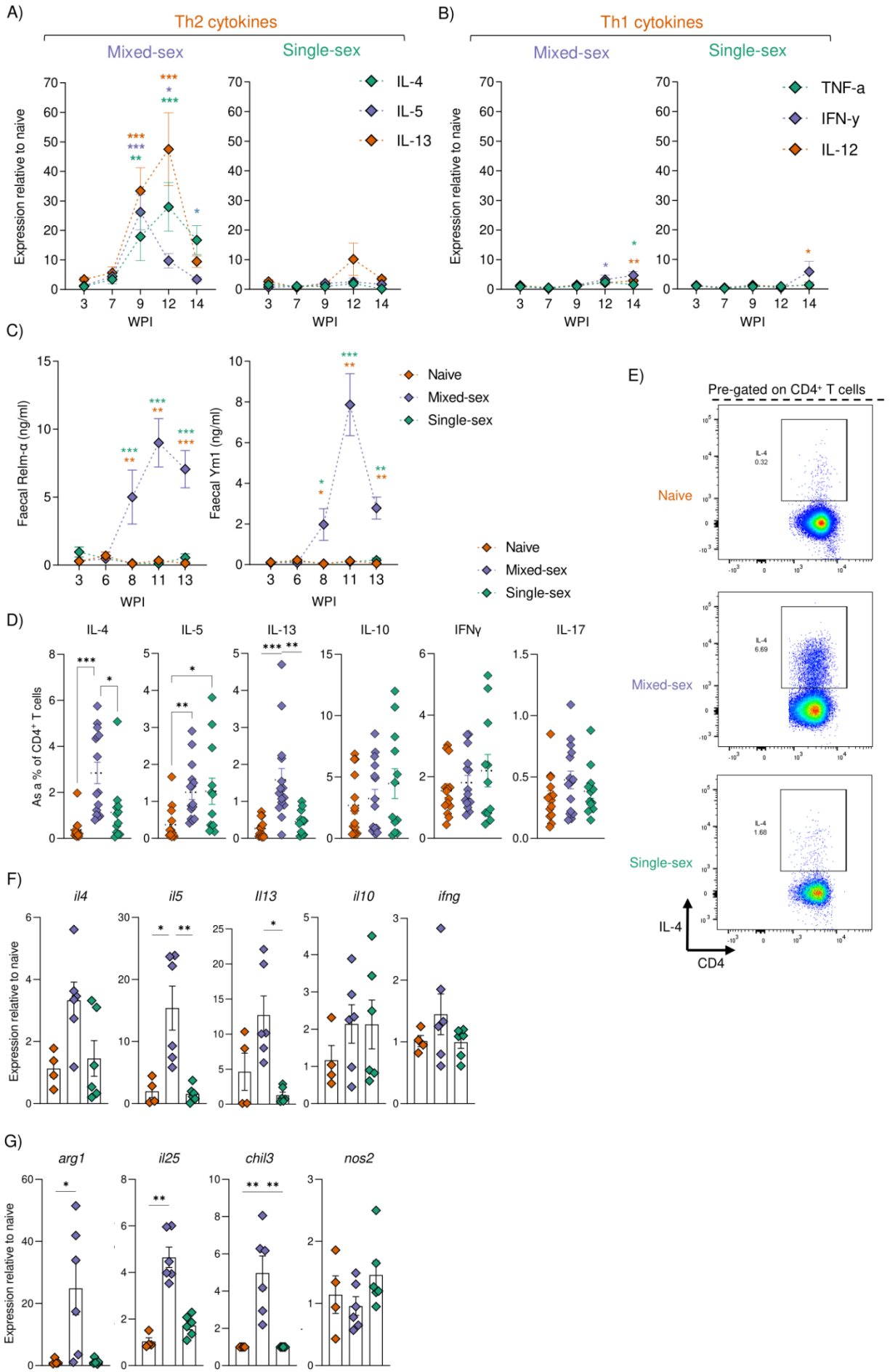
A)
Th2 cytokines
Mixed-sex
Single-sex
IL-4
IL-5
IL-13
Expression relative to naive
WPI
B)
Th1 cytokines
TNF-a
IFN-y
IL-12
C)
Faecal Relm-α (ng/ml)
Faecal Ym1 (ng/ml)
Naive
Mixed-sex
Single-sex
D)
IL-4
IL-5
IL-13
IL-10
IFNγ
IL-17
As a % of CD4+ T cells
E)
Pre-gated on CD4+ T cells
Naive
Mixed-sex
Single-sex
IL-4
CD4
F)
il4
il5
Il13
il10
ifng
Expression relative to naive
G)
arg1
il25
chil3
nos2
Expression relative to naive

Schistosome egg driven microbial disruption increases as infection progresses

Alterations in intestinal microbiota composition, as investigated through 16s rRNA sequencing, have been reported during human[39–42] and murine infections[16,17,43] with *Schistosoma spp.* including male-sex infections lacking egg production[17]. These studies either focus on one [16,17,40,42] or two isolated time points[41,43] with or without comparison into anthelminthic administration[41]. However, to our knowledge, there are no studies detailing how the microbiota changes over the course of schistosome infection and whether any changes are driven by worms, eggs or the immune response accompanying infection. To assess the influence of egg transit on microbial communities, large intestinal content was recovered from naïve, single-sex and mixed-sex infected mice at 4, 7, 12 and 14 weeks post infection, and bacterial community composition was assessed by 16s sequencing. In line with previous reports[15], intestinal microbiota profiles were comparable between experimental groups prior to the onset of egg production (4 weeks post infection), but by week 7 of infection dimensionality reduction by non-metric multidimensional scaling (NMDS) revealed a distinct shift in the bacterial composition of mixed-sex infected microbiota relative to naïve and single-sex infected groups (Figure 3A). This shift in composition became more pronounced at weeks 12 and 14 post infection suggesting that sustained egg accumulation/transit has a large influence on intestinal microbial communities. Supporting this, we observed no clear separation of naïve or single-sex samples at any time-point of infection. However, when analysed using supervised Canonical Correspondence analyses (CCA) to test whether observed trends could be explained by infection group, significant differences in colonic microbial communities became apparent between single-sex, naïve and mixed-sex infected groups (Figure 3B).

To gain insight into these microbial changes, differences in alpha diversity (Shannon diversity), richness and abundance of individual taxa was evaluated at each timepoint (Supplementary Figure 3A). While no significant differences were detected across groups at weeks 4 and 7, during chronic weeks 12 and 14, mixed-sex infections showed a significant decrease in microbial evenness without affecting either species richness or overall alpha diversity. With the above data hinting towards overgrowth or overrepresentation of particular bacterial species, we inspected bacterial communities at the genus level (Figure 3C), which revealed greater representation of bacteria of the genera *Alistipes*, *Alloprevotella*, *Bacteroides* and *Rikenellaceae* in mixed-sex infected mice at weeks 12 and 14, in comparison to earlier stages.

The intestinal microbiota plays a crucial role in host physiological processes and homeostasis, mediated in part through the vast range of metabolites they produce[44]. NMR spectroscopy was used

to capture the metabolic profile of the small intestine in naïve, single-sex and mixed-sex infected mice (Supplementary Figure 3B). Of the metabolites investigated, we observed increased levels of dihydroxyacetone in mixed-sex infected mice at week 14. Conserved across single-sex and mixed-sex infections were decreased intestinal levels of cholates and bile acids, and elevations in tartrate and lysine. We found no significant changes in intestinal levels of the short chain fatty acid butyrate.

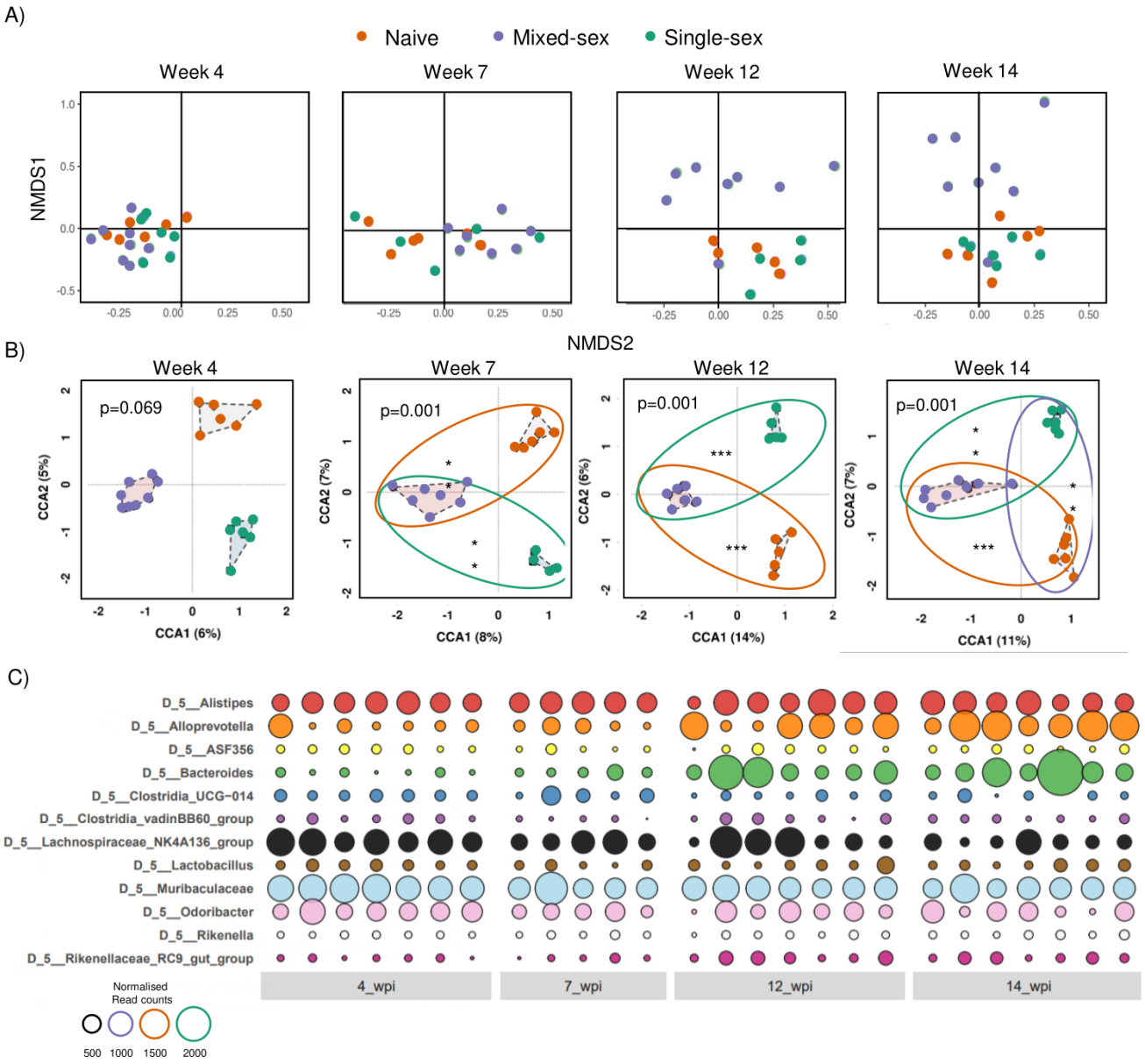

Figure 3. Egg producing schistosome infections progressively alter the of colonic microbial communities. Colonic microbial profiles of mice infected with mixed-sex or single-sex S. mansoni parasites, at weeks 4, 7, 12 and 14. Comparison made to uninfected controls. Ordinated by (A) Non-metric multidimensional scaling (NMDS) and (B) Canonical Correspondence Analysis (CCA). (C) Microbial composition at genus level in mixed sex infections only. Bubble plot representing the relative abundance of the 12 most prevalent genera. Circle diameter reflects the proportion of microbiota comprised of that genus. Empty spaces reflect no detection of a given genus by 16S sequencing. Data from one single experiment with n=5-7. Significant differences are indicated by * $p < 0.05$, ** $p < 0.01$, *** $p < 0.001$

Schistosome egg transit impairs intestinal barrier function in a dose dependent manner

Having established that egg producing infections diminish intestinal barrier function during chronic infection stages (Figure 1), we next asked how these permeability alterations could be influenced by increasing infection intensity. To test this, direct comparison was made between mice conventionally infected with 40 (low) or 180 (high) mixed sex cercariae, with infections lasting 7 weeks in duration and permeability measured 3 days prior to mouse culling (Figure 4A). As expected, high dose infected mice showed a higher burden of eggs per gram of liver tissue (Figure 4B). In line with our time-course experiment using low dose infection (Figure 1), we detected no difference in plasma FITC levels between naïve mice and those infected with 40 mixed-sex cercariae at this 6 week time-point (Figure 4C). However, significantly increased permeability was evident in mice infected with 180 cercariae at this early stage of infection, similar to low dose infected mice at later time points (i.e. week 11 onwards (Figure 1C)). Importantly, these high dose infected mice also demonstrated higher titres of commensal-bacteria specific IgG (Figure 4D) and faecal RELMα (Figure 4E) and Ym1 (Figure 4F) and increased faecal blood (Figure 4G&H). Together, these data demonstrated that intestinal barrier function was compromised to a similar degree in high dose infected mice (week 7) and mice harbouring chronic low dose infections (from week 11), and suggested that infection intensity and egg number was a strong determinant of changes in gut barrier function, rather than time after infection per se.

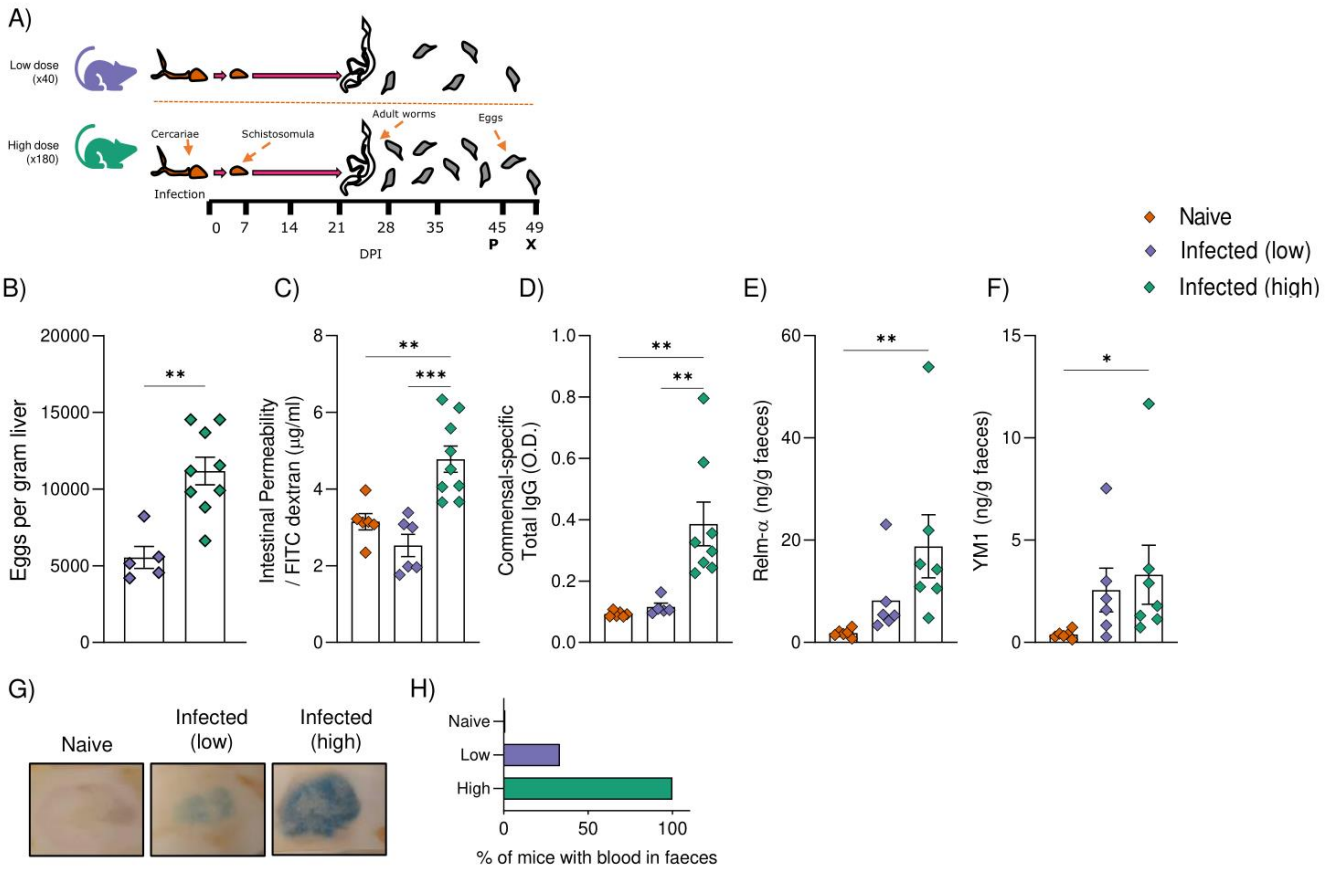

Figure 4. High dose infections evoke earlier impairments in barrier function. (A) Schematic of infection setup (weeks post infection; WPI). C57BL/5 mice were infected with 40 (low dose) or 180 (high dose) of egg producing, mixed gender S. mansoni cercariae. Infections lasted 7 weeks (indicated by X) and permeability was measured 4 days prior by FITC-dextran permeability assay (day 45). (B) Eggs per gram liver tissue (C) Changes in intestinal permeability as measured by serum FITC-dextran. (D) Serum IgG specific to commensal bacteria at week 7. (E) Faecal levels of RELMα and (F) Ym1. (G) Images depicting occult blood detection (blue) in faecal samples of indicated mice groups. (H) Percentage of mice positive for blood in faeces. Significant differences are indicated by * $p < 0.05$, ** $p < 0.01$, *** $p < 0.001$ and determined by one-way ANOVA and Tukey's post hoc test. Data presented as mean +/- SEM, * = $p<0.05$. n = 5–9 from two pooled experiments.

Immune profiles in high vs low dose infection differ more in colons than MLNs

Akin to other helminth infections[24,45] it is extremely challenging to isolate live intestinal immune cells from schistosome infected mice, with no published reports of this, and so no data available yet to assess whether MLN cellular profiles are an accurate reflection of the intestinal tissue response to schistosome infection. However, using an adapted version of recently published protocols for naïve[23] and *Heligmosomoides polygyrus* infected intestinal tissues[24,45], we were able to successfully isolate live LP leukocytes from the colons of *S. mansoni* infected mice and characterise them by multiparameter flow cytometry (Figure 5).

Irrespective of dose, we observed dramatic eosinophilia and neutrophilia in the MLNs of infected mice, alongside decreased proportions of $CD4^+$ and $CD8^+$ T cells (Figure 5A). While macrophages are typically infrequent in LNs[46], they significantly increased in both high and low dose infection groups. A clear infiltration of monocytes was observed in high dose infected mice only, while B cell frequency was moderately increased in low dose infection alone. Within the colon, we also observed significantly increased eosinophilia (low dose and high dose) and neutrophilia (high dose only) in infected mice (Figure 5B). However, in contrast to the MLNs, we observed no significant change in colonic $CD4^+$ T cell, macrophage, monocyte, or B cell frequency during infection. Taken together, similar cellular profiles were generally observed in low and high dose infection, cellular changes were generally more dramatic and evident in high dose infections, particularly in the MLN.

Having compared cellular changes in MLNs and colons from high vs low dose infection, we next investigated T cell functionality in these compartments. Focusing first on mesenteric responses, we assessed cytokine production in *ex vivo* stimulated MLN $CD4^+$ T cells (Figure 6A). Irrespective of dose, $CD4^+$ T cells from infected mice showed a significantly greater capacity to express IL-4, IL-5, IL-13, IL-10 and IFNγ than uninfected mice, and a trend towards increased IL-17. While $CD4^+$ T cells from high dose infected mice generally demonstrated a greater potential to produce these cytokines than low dose infected mice, no statistically significant difference was found. To complement these data, we evaluated MLN $CD4^+$ T cell expression of transcription factors Foxp3, Gata-3, T-bet and Rorγt, which demarcate regulatory T cells (Tregs), Th2, Th1 and Th17 cells, respectively (Figure 6B). Similar to their cytokine profiles, MLN $CD4^+$ T cells from high or low dose infection expressed higher levels of Gata-3, Foxp3 and Rorγt than uninfected controls, which was also evident for T-bet in high dose infection alone, with no significant difference between high and low dose infected mice for any of these transcription factors.

While the colonic LP contained a relatively low percentage of CD45$^+$ cells (~10-20% of total), sufficient numbers were recovered to characterise the CD4$^+$ T cell compartment (Figure 6C&D). In clear contrast to the comparable phenotype of MLN CD4$^+$ T cells isolated from high vs low dose infection, only colonic CD4$^+$ T cells from high dose infection had a significantly increased capacity to produce IL-5, IL-13, IL-10 and IFNγ in comparison to naïve mice, and a trend towards higher IL-4 (Figure 6C)**.** Similarly, colonic CD4$^+$ T cell expression of Gata-3 and T-bet was increased in high dose infections only (Figure 6D), and no significant differences in Foxp3 or Rorγt were detected.

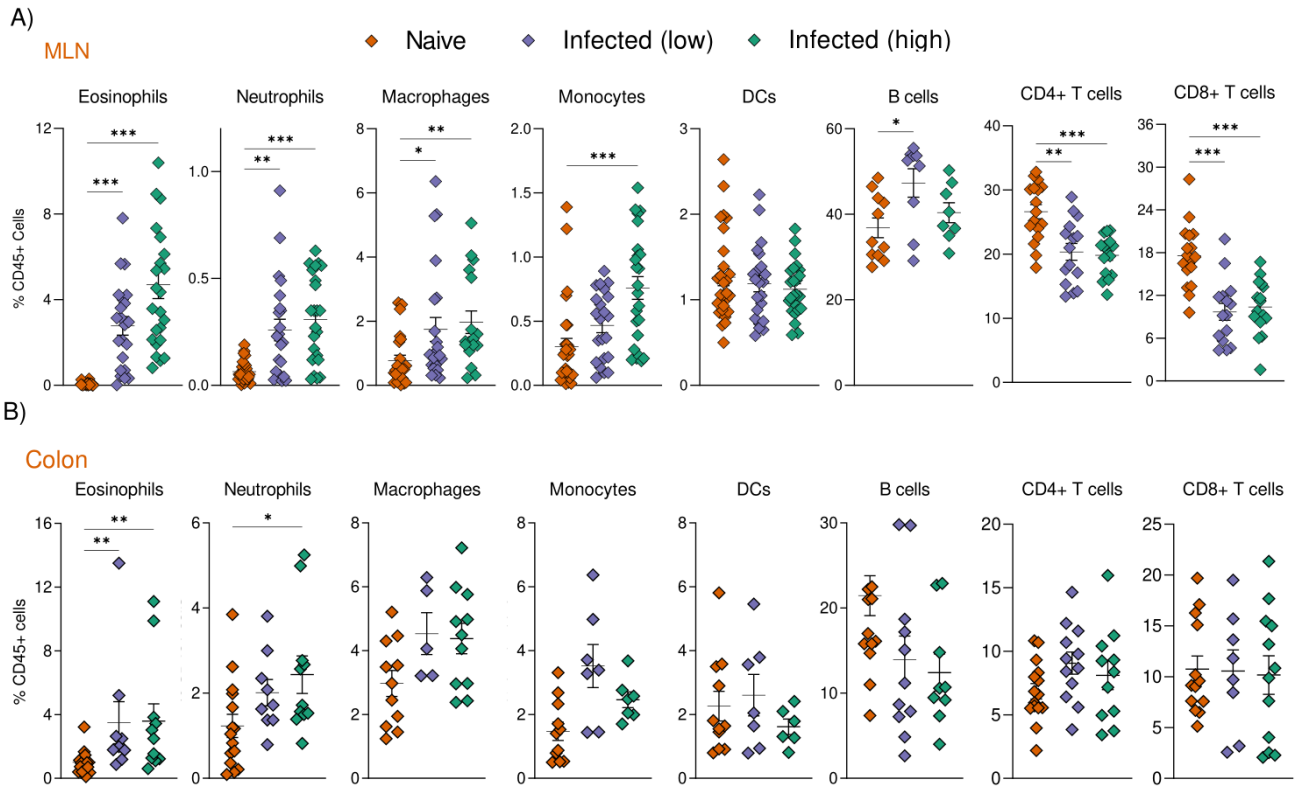

Figure 5. Increased appearance of granulocytes in colon and MLN of schistosome infected mice. The frequency of various immune cells in the (A) MLN and (B) colon of schistosome infected mice. Data shown are from 7 (A) or 5 (B) pooled experiments, with 2-4 mice per experimental group per experiment. Data presented as mean +/- SEM. Significant differences were determined by one-way ANOVA with suitable post-hoc testing. *p < 0.05, **p < 0.01, ***p < 0.001

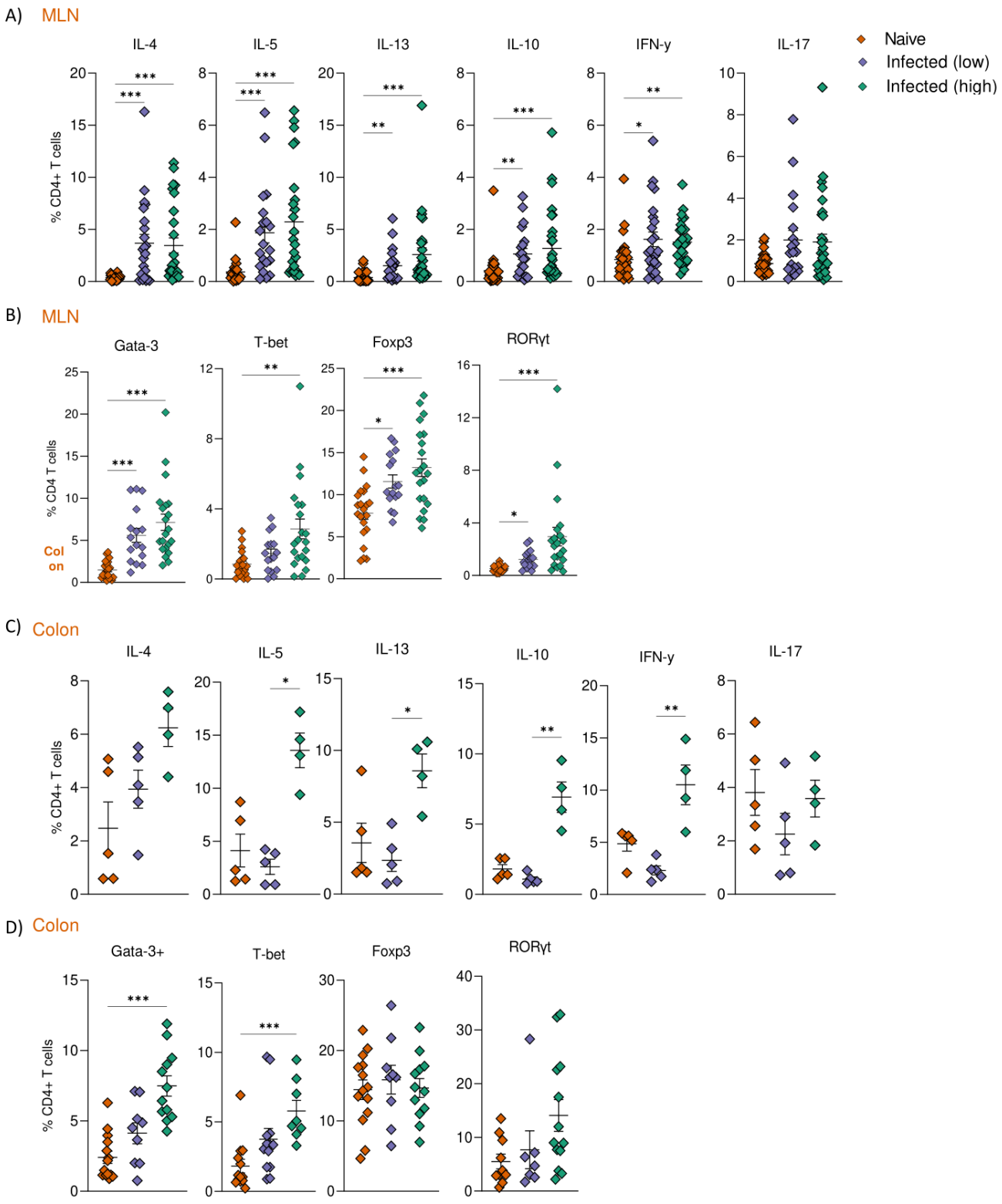

Figure 6. T cell profiles differ between infection doses in the colon. Cytokine secretion from PMA ionomycin stimulated (A) MLN and (C) colonic CD4+ T cells. The expression of Th1 (T-bet), Th2 (Gata-3), Th17 (Rorγt) and Treg (Foxp3) associated transcription factors in (B) MLN and (D) colonic CD4+ T cells. Data presented as mean +/- SEM. Data shown are from 2 (C), 3 (4) or 7 (A&B) pooled experiments n= 2-4 per experimental group per experiment. Significant differences were determined by one-way ANOVA with Tukey post hoc testing. *p < 0.05, **p < 0.01, ***p < 0.001

Egg driven microbial alterations are dose dependent

Having demonstrated accelerated intestinal permeability and damage (Figure 4), along with more marked intestinal immune responses (Figures 4-6), in high vs low dose infection, we next addressed the impact of infection dose on bacterial community structure. 16s sequencing was performed on the large intestinal content of naïve mice and those infected for 7 weeks with 40 or 180 schistosome parasites (Figure 7). As expected, schistosome infection, irrespective of dose, evoked shifts in colonic bacterial communities with visualisation of clustering by PCoA showing clear separation between naïve, low dose and high dose infected mice (Figure 7A). When analysed by CCA, a significant difference in microbial profiles was detected between naïve and high dose infected mice but, due to a shortage of numbers, statistical testing was not possible for low dose groups (Figure 7B). A significant decrease in alpha diversity (quantified by Shannon index) was observed in high dose infection, with a trend towards lower species richness and abundance (Figure 7C).

With the data indicating a more marked impact of high dose infection on the host microbiota, we next assessed how infection altered bacterial communities at the genus level. Looking first at the 12 most abundant bacterial genera (Figure 7D), high dose infection led to an outgrowth of *Staphylococcus* and *Lachnospiraceae NK4A136* in comparison to low dose infected and uninfected mice. *Bacteroides*, *Alistipes* and *Biophilla* were also expanded upon infection but irrespective of infection dose. Mixed-sex infected mice at week 12 and 14 also showed greater representation of *Bacteroides* and *Alistipes* (Figure 3C), suggesting a conserved effect of heavy egg burden.Focusing on the more significant alterations in bacterial genera between groups (Figure 7E), high dose infection led to a decline in the abundance of *Muribacterium, RF39*, *Parasutterlla*, while bacteria of the genera *Ruminatium*, *Siraeum Dubosiella* and *Runmioccocus* were now undetectable in the colonic content of high dose infected mice.

We next sought to characterise the small intestinal metabolomic profile associated with high and low dose infection (Supplementary Figure 4) and saw a general trend towards decreased levels of certain amino acids (isoleucine, leucine, methionine and sarcosine) and metabolites associated with liver function (bile acids and cholates) in infected mice. This trend towards reduced bile acids and cholate mirrors that observed in our low dose time course experiment (Figure 3B).

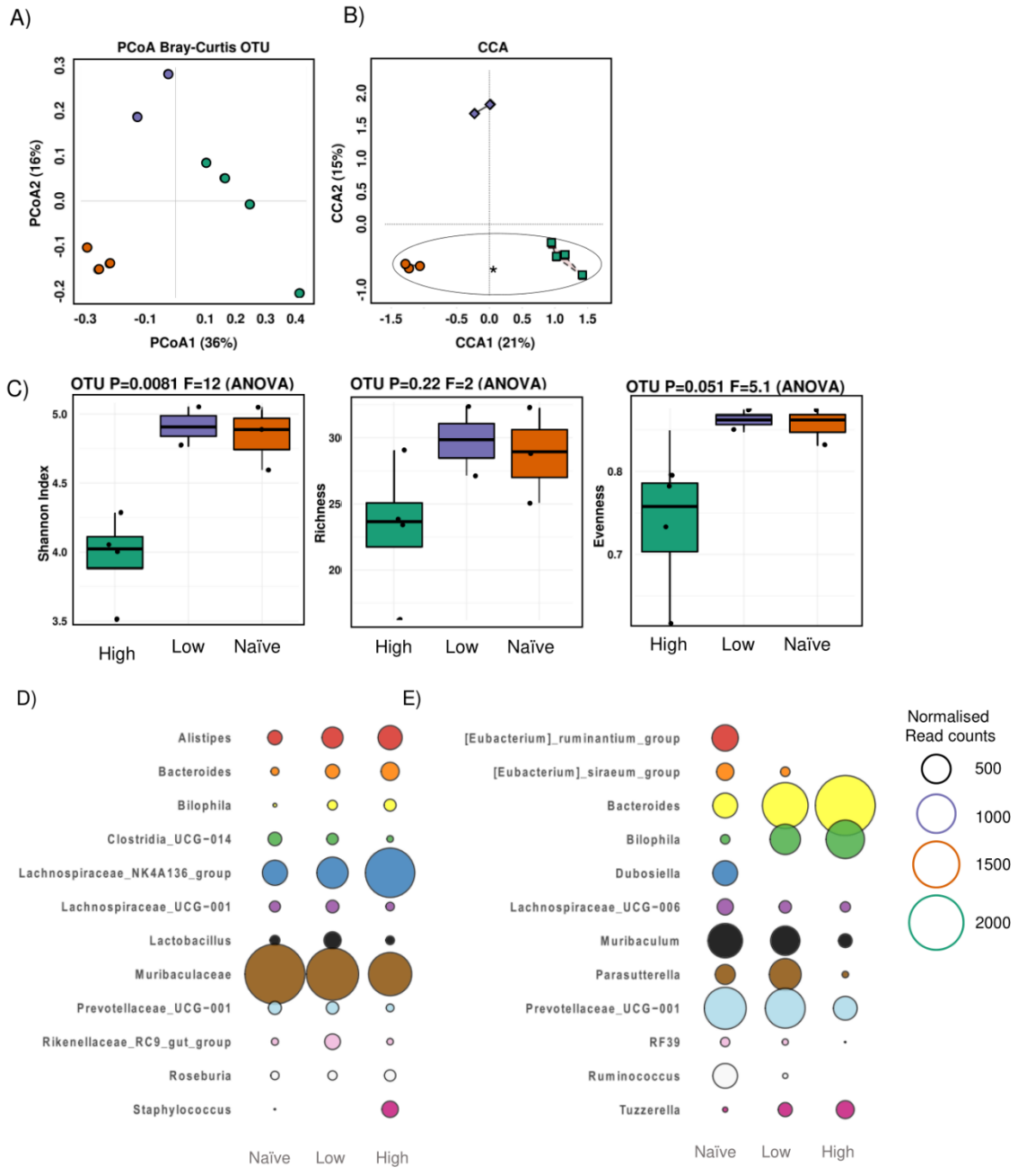

Figure 7. Schistosome infections provoke dose dependent dysbiosis. Colonic microbial profiles in low and high dose infected mice at week 7 of infection, as displayed as (A) Principal Coordinate Analysis (PCoA) and (B) Canonical Correspondence Analysis (CCA). (C) Alteration in microbial alpha as measured by species evenness, abundance and Shannon diversity. (D) Bubble plots representing the relative abundance of the (D) 12 most prevalent genera or (E) 12 genera showing the largest fluctuations between groups. Circle size reflects the proportion of microbiota comprised of that genus. Empty spaces reflect no detection of a given genus by 16S sequencing. Data from one single experiment with n=2-4. Significant differences are indicated by * $p < 0.05$, ** $p < 0.01$, *** $p < 0.001$

Transfer of schistosome infection-associated microbiota into GF recipients promotes MLN CD4$^+$ T cell IL-4 production

After identifying pronounced differences in immune profiles and intestinal microbiota compositions between naïve mice and those infected with egg producing schistosomes, we next sought to directly address the relationship between the two. More specifically, we questioned whether the schistosome infection-associated microbiota contributes to intestinal immune polarisation. GF C57BL/6 mice were colonised for 2 or 3 weeks with defined microbiotas by transfer of faeces from SPF mice that had been infected with *S. mansoni* for 7 weeks, or from naïve controls (Figure 8A) and characterised the microbiota of recipient mice by 16s rRNA sequencing (Supplementary figure 5A). Given the relatively comparable immune profiles observed between low and high dose infected mice, faeces were pooled across infection groups to generate the faecal transplant 'slurry'. Strikingly, mesenteric CD4$^+$ T cells from mice recolonised with a schistosome infection-associated microbiota expressed significantly more of the Th2 associated cytokine IL-4 than mice receiving naïve faeces or PBS alone (Figure 8 B&C)**.** This trend could not be recapitulated with gavage of schistosome eggs alone (Supplementary Figure 5B) CD4$^+$ T cells from the same experimental group also trended towards greater IL-17 production, while secretion of IL-5, IL-13, IL-10 and IFNγ was comparable between groups. As faeces was pooled from high and low dose infected mice, we cannot distinguish which microbiota is the MLN IL-4 inducing trigger. However, given the preceding permeability (Figure 4) and immune (Figure 5&6) we anticipate these effects to be associated with high dose microbiotas.

Although IL-4 was increased in MLN CD4$^+$ T cells from GF mice that received faeces from schistosome infected mice, the expression of the Th2 defining transcription factor GATA-3 was comparable in those cells across experimental groups (Figure 8D). However, we noted a significantly increased frequency of Rorγt$^+$ CD4$^+$ T cells, and decreased Foxp3$^+$ CD4$^+$ T cells, in MLNs of mice colonised with schistosome infection-associated microbiotas (Figure 8D). Finally, irrespective of donor, faecal transplant failed to have a significant impact on the proportion of myeloid or granulocytic cells in the MLN of recipient GF mice, with the exception of monocytes, whose frequency was significantly enhanced upon receipt of a schistosome infection associated microbiota (Supplementary Figure 5C). Numerically, faecal transfer recipients tended towards greater MLN counts than PBS controls, which was reflected by significantly higher absolute counts of eosinophils, monocytes and plasmacytoid dendritic cells (pDCs) (Supplementary Figure 5D).

Together, these data reveal that recolonisation of GF mice with the microbiota associated with schistosome infection is sufficient to induce IL-4+ CD4+ T cells in the MLNs of recipient mice.

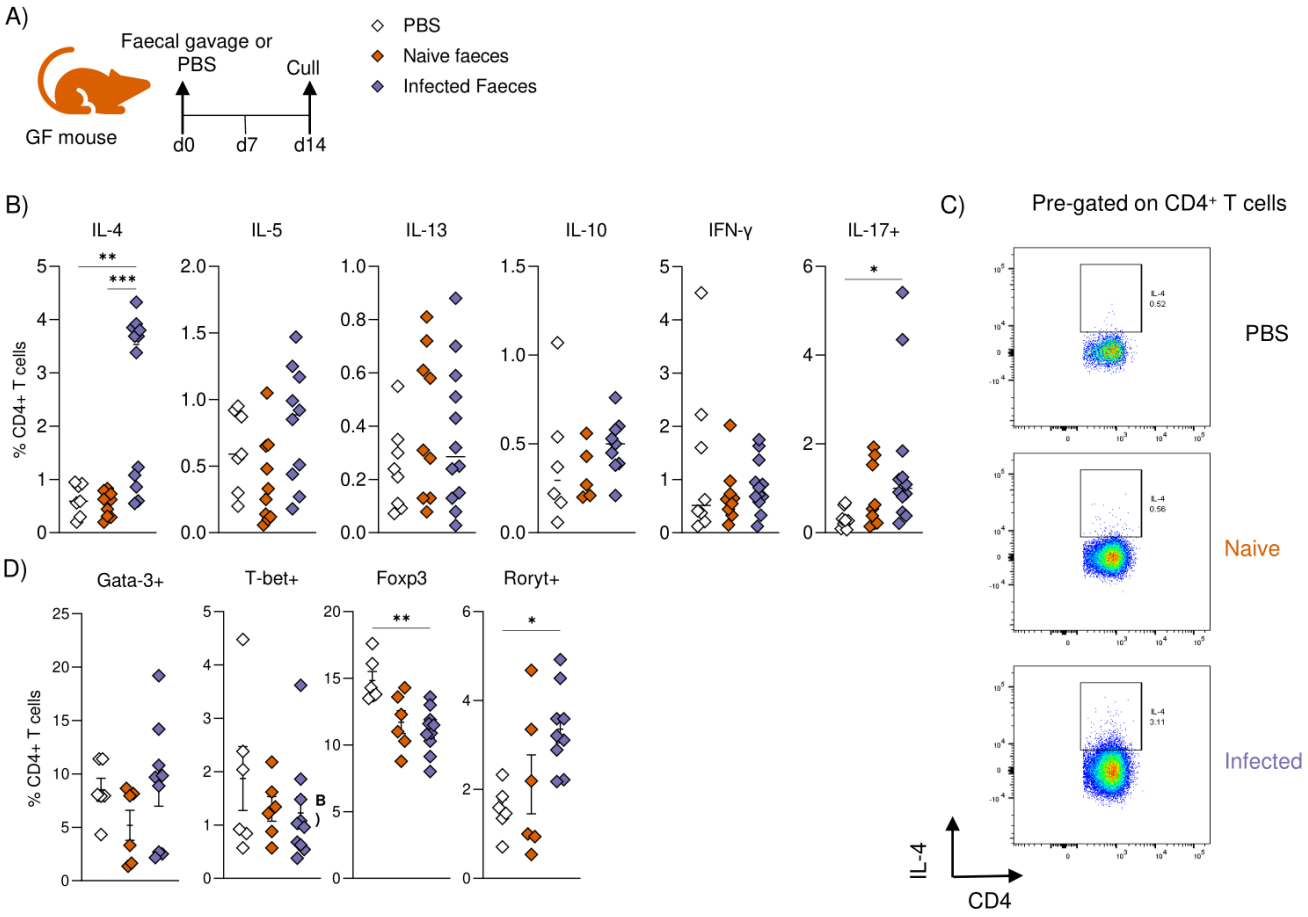

Figure 8. Transfer of faeces from schistosome infected mice into germ free mice evokes local Th2 and Th17 response. (A) Experiment schematic. Germ free mice were colonised for 2 or 3 weeks with faeces from naïve or mice infected with schistosomes for 7 weeks. Faeces was pooled from high and low dose infected mice for the generation of the 'infected' faecal slurry. (B) Cytokine secretion from PMA ionomycin stimulated CD4+ T cells. (C) Representative flow plots for IL-4 secretion, pre-gating on live CD45+ TCRβ+ CD4+ cells. (D) The expression of Th1 (T-bet), Th2 (Gata-3), Th17 (Rorγt) and Treg (Foxp3) associated transcription factors in MLN CD4+ T cells. Data presented as mean +/- SEM. Data pooled from two (D) or three pooled experiments. n=6-13 mice per group. Significant differences were determined by one-way ANOVA followed by Tukey's post hoc test. *p < 0.05, **p < 0.01, ***p < 0.001.

Schistosomes, like many helminths, are renowned for their capacity to modulate the host immune response[10,47]. This includes their ability to limit collateral tissue damage to the host, regulate immunity towards bystander Ags and promote immune environments that enable their longevity[1410]. Despite the continuous transit of schistosome eggs across the intestinal tissues, and the damage this process causes, we currently lack understanding as to how egg-driven intestinal responses are regulated, and how local immune responses and commensal microbes influence these processes. Here we have directly investigated the impact of schistosome egg production on intestinal barrier function, local immune polarisation, and colonic bacterial communities by comparing mixed-sex vs single-sex, and high vs low dose, *S. mansoni* infections. We show that egg production is central to intestinal damage and permeability, cytokine production, and altered microbiome, with levels of each of these outcomes dictated by chronicity and/or intensity of infection. By transferring faeces from mixed-sex *S. mansoni* infected SPF donor mice into GF recipients, we have discovered the ability of the schistosome infection-associated microbiota to direct host MLN $CD4^+$ T cells towards a Type 2 phenotype. Together, these data suggest an active role for the intestinal microbiota, shaped by the egg stage of the parasite, in priming host intestinal immunity during schistosomiasis.

Previous researchers have suggested that a 'leaky gut' and subsequent luminal content exposure may[48–51], but this has never been directly tested. Here, we provide the first evidence that altered barrier integrity during schistosomiasis influences the immune trajectory of the host. Intestinal permeability was increased during chronic and high-intensity *S. mansoni* infections, with evidence of barrier damage from the onset of egg production (Figures 1&4). While in murine low dose infections permeability was evident by week 11 of infection, in high dose infections alterations could be visualised as early as week 6. These data highlight the resilience of the intestinal barrier and indicate that although egg migration provokes intestinal damage from the onset, sustained egg accumulation or high intensity production is required for intestinal leakiness to become evident. In addition, it is possible that in high dose settings, the intestines recuperative capacities are overwhelmed, leading to earlier permeability changes. Extrapolating this data to a human setting, we anticipate that these permeability alterations may take longer to manifest, reflecting sheer size differences in mouse-human anatomy. Individuals hyper-exposed to *S. mansoni* (i.e fisherman in endemic regions) display significantly higher endotoxemia in comparison to uninfected persons[52]. While these data imply enhanced intestinal permeability in infected persons, this has not been

addressed through more direct methods of assessment (i.e oral gavages with saccharides[53,54]) and the kinetics of these changes are unknown.

It is important to note that, although we focussed on the influence of egg migration on paracellular permeability (i.e movement between adjacent epithelial cells), luminal content can cross the epithelium via other means. This includes specialised microfold (M) cells that overlay specialised lymphoid follicles, and the extension of dendritic cell (DC) dendrites through the epithelial layer[55]. Although not directly assessed here, it is plausible to suggest that egg migration disrupts the homeostatic function of these cell types/processes, resulting in altered Ag uptake via these routes. Similarly, Ag uptake could be facilitated by increased cellular apoptosis and epithelial cell turnover[17]. Finally, with high-level mucus production hallmarking helminth infections[56,57] it is possible that mucin-producing goblet cells act as conduits for DC Ag delivery, in a process known of retrograde endocytosis[55,58]

Schistosomes are not the only parasites known to damage the intestinal barrier during their infectious life-cycles, including *Toxoplasma gondii*, *H. polygyrus* and *Fasciola hepatica*[59]. Despite the physical damage they impose on the gastrointestinal tract, none of these infections are typically associated with sepsis or secondary bacterial infection[59], even though schistosome-infected individuals are reported to have systemic endotoxin levels at 10 times greater than that observed in lethal toxic shock[52]. This enigma may reflect a greater capacity of the host immune system to deal with these high LPS burdens, as observed in F. hepatic infections[60,61], or immune hyporesponsiveness in chronic disease[62]. Additionally, this could be due to the dynamic regenerative capacity of the intestinal tissues, counteracting parasite-evoked damage and generating a robust mucosal immune response that limits bacterial spread[59.] Given that host survival is vital for the parasite, they likely manipulate host immune responses in a manner that improves bacterial control, and thus their own longevity. Indeed, chronic filarial infections have shown to promote bacterial clearance and sepsis survival via the functional reprogramming of macrophages[63.] How schistosomes prevent sepsis is relatively uncharted research. One molecule that warrants attention includes cDC2 -derived hepcidin, which was recently shown to promote intestinal wound healing and limit microbiota tissue infiltration following DSS challenge[64]. In addition, resident macrophage populations in the liver (Kupffer cells) have recently been shown to be crucial for the capture of intestinal bacteria and prevention of their dissemination[65]. Given the large impact of schistosomiasis on host liver function, further studies to assess this mechanism are warranted.

The capacity to isolate live immune cells from the intestine of schistosome infected mice (Figure 5&6) brings forth many exciting opportunities. Here, we provide a broad snapshot into schistosome-evoked immunity within the intestine, and thus, there remain many fascinating avenues of adaptive and innate immunity still open for exploration. For example, macrophages play important roles in the promotion or resolution of tissue damage, where surrounding cytokine environments dictate their 'M1' proinflammatory or 'M2' wound healing capacities[38]. Considering the intestinal tissue damage evoked by *S. mansoni* infection (Figures 1&4), schistosome infections represent a compelling system to unearth the core cell types and effector molecules that regulate mucosal inflammation, and the signals underlying their generation. Colonic macrophage frequencies were comparable between high and low dose infected mice (Figure 5), but their relative activation and M1/M2 status was not evaluated. Refined assessment of M2/pro-repair factors (e.g Ym1/2, Relmα Arginase) vs M1/pro-inflammatory (iNOS, TNF) factors would be of particular interest here. Such high dimensional flow analysis, paired with techniques of RNA seq and imaging mass cytometry, and analysis across the whole course of infection, would provide an unprecedented image into the schistosome intestine. Inclusion of in situ hybridization, could also provide insight into the localisation of infiltrating bacteria relative to immune cells and sites of damage[100].

While MLN immune profiles were similar between low dose and high dose infected mice (Figure 5&6), we observed dose dependant differences in PMA/ionomycin stimulated cytokine secretion (Figure 6), with high dose infected mice producing greater levels of IL-5, IL-10, IL-13 and IFNγ than low dose infected mice. These results suggest that while LN priming of $CD4^+$ T cells is comparable between the two infection intensities, their colonic environments vary and differ in their capacity to support or maintain T cell polarisation. This may reflect differences in colonic egg burden or exposure to damage or luminally-derived products. Instalment of cytokine reporter mice, or conduction of e*x vivo* SEA and commensal bacteria specific stimulation will provide further clarity on this matter.

The composition of the intestinal microbiota is intricately linked to the fine tuning of host immunity, with GF mice showing stunted immune development[66] and skewed Th2 responses[67], and with certain microbial species shown to endorse the conversion of naïve $CD4^+$ T cells into immunosuppressive Tregs[68,69] or more proinflammatory Th17 cells[70]. Here we reveal the capacity of the schistosome infection-associated microbiota to boost mesenteric $CD4^+$ T cell production of IL-4 and induce the appearance of $CD4^+$ T cells with a greater expression of $Ror\gamma t^+$ (Figure 8). While previous research has shown bacterially-derived molecules to reverse the Th2 'bias' observed in GF

animals[67], to our knowledge this is the first report demonstrating the ability of infection to promote resident microbes that enhance intestinal T cell IL-4 production. As our analysis showed no significant increase in $CD4^+$ T cell IL-5, IL-13, IL-10 or GATA-3 expression (Figure 8), our data may indicate the generation of T follicular helper (Tfh) cells that are pre-primed for release of IL-4[71] . Alternatively, our data could suggest for a transient wave of Type 2 immunity, which has been described in the developing lung at maximum periods of lung remodelling[72,73]. In these pulmonary studies, Type 2 innate immune cells flux into the lungs in response to rising IL-33 and display a lower threshold for responses towards allergens[73]. Thus, it would be of particular interest to inspect IL-33 and Tfh levels in our experiments, with use of IL-4 reporter mice providing greater insight into the contribution of individual $CD4^+$ subsets to the IL-4 pool. Finally, comparison of high dose and low dose microbiotas, or mixed-sex vs single-sex microbiotas is also warranted, with this analysis highlighting whether the MLN IL-4 phenotype is exclusive to particular doses or time points of *S. mansoni* infection.

In the context of schistosomiasis, where the generation of an appropriately regulated Th2 responses underpins host survival[48,49,51], the ability of the host immune system to rapidly respond to recurring infection would be of immediate benefit. In support of this line of reasoning, certain *Lactobacillaceae* species have shown to prime host immunity in a manner that alters susceptibility to enteric helminth *H. polygyrus*[74]. Moreover, susceptibility to schistosomiasis has shown partial dependence on baseline microbiota composition[16,19], and the degree of schistosome evoked granulomatous inflammation can be altered through antibiotic administration[20]. Future studies should address the relevance of commensal driven MLN IL-4 populations to barrier repair or promotion of Type 2 immunity, for instance by challenging faecal transplant recipients with *S. mansoni* or models of colitis.

The induction of Th17 cells by the intestinal microbiota has primarily been accredited to segmented filamentous bacteria (SFB)[70], but may also involve other commensals[75]. Th17 responses are not typically associated with schistosomiasis infections in C57BL/6 mice[76], but in CBA/J mice, they are associated with severe egg-driven pathology[77]. Although we did not see significantly increased Th17 development in our infection experiments, our observation that MLN $ROR\gamma t^+$ $CD4^+$ T cell responses were somewhat elevated in high dose infection (Figure 5) or following faecal transplant from high dose infection into naïve GF mice (Figure 8), suggests that this immune phenotype may be conferred by a component of the schistosome infection-associated microbiota, caused by egg transit and tissue damage. In support of this idea, schistosome infection-associated microbiotas have shown to

be pro-inflammatory/ 'colitogenic' in co-housing studies[78], and inflammatory IBD associated microbiotas are accompanied by an abundance in mucosal Th17 cells and a disproportionate ratio of Tregs[79]. Furthermore, given the crucial role of Th17 cells in maintenance of intestinal barrier function and compartmentalisation of the intestinal microbiota[80], perhaps the promotion of mucosal RORγt$^+$ CD4$^+$ T cell responses by the schistosome microbiota represents a conserved evolutionary mechanism that could help fortify the intestinal wall against egg transit. Finally, it is plausible to suggest that the microbiota-instructed RORγt$^+$ T cells may play a role in the regulation of Type 2 immunity[81]

It remains unclear which particular microbial species, metabolites or global changes within the intestinal system may be responsible for the development of MLN IL-4$^+$ and RORγt$^+$ CD4$^+$ T cells in faecal transplant mice (Figure 8). Similarly, it is unknown whether certain microbial components contribute to barrier integrity and repair during egg transit. While 16s sequencing revealed structural differences between faecal transplant recipients (Supplementary Figure 5), and naïve or infected mice (Figures 3&7), this analysis was not capable of fully capturing the metabolic activity or functionally of the identified groups. For instance, we observed conserved expansion of *Bacteroides* and *Alistipes* genera across chronic (12-14 week) low dose mixed-sex and 7 week high dose mixed-sex infections (Figures 3&7). However, with some species within these genera showing pro-inflammatory[82,83] potential, and others showing anti-inflammatory[83,84] effects, it remains unclear how these bacterial modifications impact the outcome of *S. mansoni* infection. Shotgun metagenomic sequencing provides taxonomic resolution at a species level, offers information on their functional potential, and allows characterisation of fungal and viral communities. Integrating this approach with metabolomic analysis, alongside inspection of microbiotas from different regions of the intestine, would provide further clarity on microbial factors responsible for the observed immune phenotype. Furthermore, with advances in culturomics and metagenomics, it may soon be possible to identify and capture candidate bacteria and move away from cruder faecal transplant work.

Enteric helminths disrupt microbiota composition through a variety of approaches[14], including the anti-microbial activity of their extracellular secretary (ES) products, competing with microbial species for nutrients and the intestinal niche, and altering mucin dynamics and so settlement of certain mucin-colonising bacteria[85–87]. Our data reveals a clear-cut role for egg transit in schistosome infection-associated modification of host microbiota structure, with egg-driven microbial alterations shown to increase over the course of infection (Figure 3), and differences in bacterial communities

also more dramatic with increasing infection dose (Figure 7). However, it remains unclear whether these bacterial changes reflect the secretion of antimicrobial compounds from schistosome eggs, the Th2 dominated immune response associated with infection, or the destructive inflammatory response evoked by egg transit. Our data generally supports egg-driven tissue damage as the dominant candidate for altering the host microbiota. More specifically, by comparing chronic low dose mixed-sex and post-patent acute high dose mixed-sex infections, we revealed significant impairment in barrier function associating only with later timepoints in low dose infections (Figure 1), and only with high dose post-patent acute infections (Figure 4), even though clear Type 2 immune responses were present earlier or in low intensity infections (Figures 2&5). The association of infection chronicity and/or intensity with intestinal damage was also evident for changes in microbial profiles (Figures 3&7). Mechanistically, a higher level of egg transit likely exposes cells within damaged tissues to several forms of stress, leading to enhanced necrosis and apoptosis[17], and potential release of endogenous danger molecules, which may then generate an intestinal niche that favours certain microbes. It is important to note that, although intestinal leakiness increased with chronicity or intensity of mixed-sex infections, the intestinal barrier appeared intact through histological inspection and analysis of tight junction associated genes (Supplementary Figure 1B). Thus, the intestine during schistosomiasis is able to rapidly heal several aspects of egg-associated damage, through mechanisms that remain to be determined. It is possible that these processes may involve the host microbiota, given that some intestinal bacteria can promote wound healing[88]. In terms of immune-mediated modifications to the microbiota, Type 2 immune responses may promote the expulsion or expansion of defined intestinal bacteria, as already show in in the context of murine infection with *Trichuris muris* infecton[89] or *H. polygyrus*[90]. In the context of our work, this could in part be facilitated by schistosome infection increasing Th2 associated mediators such as Ym1 and RELMα in the luminal content (Figures 2&4), anti-commensal antibodies (Figures 1&4), or IL-25 production – all of which could influence intestinal epithelial cells and IL-13 responses[91]**.** Additionally, RELMα has shown bactericidal effects within the skin[92], but its intestinal antibacterial properties are uncharacterised. Similarly, antimicrobial peptides and proteins (AMPs) induced by helminth infection could selectively tailor the host microbiota and modify their tissue location[90]. Moreover, it is possible that an impaired barrier function alters sampling of gut bacteria by innate immune cells, leading to modified inflammation, IgA induction and capacity to compartmentalise the microbiota[93].

In addition to schistosome eggs, the fact that single-sex infections are associated with changes in the intestinal microbiota by week 14 (Figure 3) indicated that the worms alone, even though they

live in the mesenteric vasculature, can impact the composition of the intestinal microbiota. Indeed, intestinal microbiota alterations has been reported in individuals infected with the urogenital parasite, S. haematobium, which are distally located within the bladder plexus[18,39]. Additionally, helminth-derived secretions have shown to elicit direct antimicrobial activities[94], though this has not yet been investigated for schistosomes. However, given that single-sex infections were also accompanied by small but significant elevations in systemic and local Th1 mediators at the 14 week timepoint (Figure 2 & Supplementary Figure 2) where we observed concurrent changes in the intestinal microbiome (Figure 3), our data likely indicate immune involvement as opposed to the direct actions of the worm secretions, which will have been produced throughout infection.

We have found that schistosome infection not only impacts intestinal microbial composition, but also has consequences in terms of metabolites (Supplementary Figures 3&4). Alterations in the intestinal metabolome may reflect differences in host, parasite and/or bacterial production or utilisation of metabolites, as well as their absorption across the intestinal wall[95]. Of particular interest, in both single-sex and mixed-sex infections we detected significant reductions in levels of bile acids and cholates within the small intestine (Supplementary Figure 3). Recent studies have pinpointed a role for bile acids in shaping the composition of intestinal immune populations[96,97],including the promotion of haemopoiesis and subsequent conferred protection against infection[98]. While the alterations in bile acids may reflect schistosome worms influencing liver function, it is possible this may also have a role in shaping schistosome associated immune responses, and the ability of the host to fight off concurrent infections or leakage of intestinal derived Ags or pathogens across the intestinal wall[99].

In conclusion, we have identified profound alterations in barrier integrity, immune polarisation, and colonic microbial structure over the course of murine schistosomiasis, with changes coinciding with chronicity and/or intensity of intestinal tissue-damaging parasite eggs. Additionally, we have shown that the schistosome infection-associated microbiota promotes development of MLN IL-4$^+$ and RORγt$^+$ CD4+ T cells, which may be of further consequence or benefit to parasite and host survival. This work provides a robust experimental platform for further interrogation, and discovery of novel mechanisms that link parasite, microbial and immune factors to 'regulated' intestinal inflammation.

REFERENCES

1. McManus, D. P. *et al.* Schistosomiasis. *Nature Reviews Disease Primers* **4**, 1–19 (2018).
2. Costain, A. H., MacDonald, A. S. & Smits, H. H. Schistosome Egg Migration: Mechanisms, Pathogenesis and Host Immune Responses. *Frontiers in immunology* **9**, 3042 (2018).

3. Dunne, D. W. & Pearce, E. J. Immunology of hepatosplenic schistosomiasis mansoni: A human perspective. *Microbes and Infection* **1**, 553–560 (1999).
4. Secor, W. E. *et al. Association of Hepatosplenic Schistosomiasis with HLA-DQBl *0201*. *academic.oup.com* (1996).
5. Mohamed-Ali, Q. *et al.* Susceptibility to Periportal (Symmers) Fibrosis in Human *Schistosoma mansoni* Infections: Evidence That Intensity and Duration of Infection, Gender, and Inherited Factors Are Critical in Disease Progression. *The Journal of Infectious Diseases* **180**, 1298–1306 (1999).
6. Costain, A. H., MacDonald, A. S. & Smits, H. H. Schistosome Egg Migration: Mechanisms, Pathogenesis and Host Immune Responses. *Frontiers in immunology* vol. 9 3042 (2018).
7. Everts, B. *et al.* Omega-1, a glycoprotein secreted by Schistosoma mansoni eggs, drives Th2 responses. *Journal of Experimental Medicine* **206**, 1673–1680 (2009).
8. Haeberlein, S. *et al.* Schistosome egg antigens, including the glycoprotein IPSE/alpha-1, trigger the development of regulatory B cells. *PLoS Pathogens* **13**, e1006539 (2017).
9. Straubinger, K. *et al.* Maternal immune response to helminth infection during pregnancy determines offspring susceptibility to allergic airway inflammation. *Journal of Allergy and Clinical Immunology* **134**, 1271-1279.e10 (2014).
10. Maizels, R. M., Smits, H. H. & McSorley, H. J. Modulation of Host Immunity by Helminths: The Expanding Repertoire of Parasite Effector Molecules. *Immunity* vol. 49 801–818 (2018).
11. Vicentino, A. R. R. *et al.* Emerging Role of HMGB1 in the Pathogenesis of Schistosomiasis Liver Fibrosis. *Frontiers in Immunology* **9**, 1979 (2018).
12. Everts, B., Smits, H. H., Hokke, C. H. & Yazdanbakhsh, M. Helminths and dendritic cells: Sensing and regulating via pattern recognition receptors, Th2 and Treg responses. *European Journal of Immunology* vol. 40 1525–1537 (2010).
13. Maizels, R. M. *et al.* Parasitic helminth infections and the control of human allergic and autoimmune disorders. *Clinical Microbiology and Infection* **22**, 481–486 (2016).
14. Brosschot, T. P. & Reynolds, L. A. The impact of a helminth-modified microbiome on host immunity. *Mucosal Immunology 2018 11:4* **11**, 1039–1046 (2018).
15. Jenkins, T. P. *et al.* Schistosoma mansoni infection is associated with quantitative and qualitative modifications of the mammalian intestinal microbiota. *Scientific Reports* **8**, 12072 (2018).
16. Cortés, A. *et al.* Baseline Gut Microbiota Composition Is Associated With Schistosoma mansoni Infection Burden in Rodent Models. *Frontiers in Immunology* **11**, 1 (2020).
17. Floudas, A. *et al. Schistosoma mansoni* Worm Infection Regulates the Intestinal Microbiota and Susceptibility to Colitis. *Infection and Immunity* **87**, (2019).
18. Ajibola, O. *et al.* Urogenital schistosomiasis is associated with signatures of microbiome dysbiosis in Nigerian adolescents. *Scientific Reports* **9**, 829 (2019).
19. Viera, L. Q. & Moraes-Santos, T. Schistosomiasis mansoni: evidence for a milder response in germfree mice. *Revista do Instituto de Medicina Tropical de São Paulo* **29**, 37–42 (1987).
20. Holzscheiter, M. *et al.* Lack of host gut microbiota alters immune responses and intestinal granuloma formation during schistosomiasis. *Clinical & Experimental Immunology* **175**, 246–257 (2014).
21. Janse, J. J. *et al.* Establishing the production of male schistosoma mansoni cercariae for a controlled human infection model. *Journal of Infectious Diseases* **218**, 1142–1146 (2018).
22. van Dam, G. J., Bogitsh, B. J., van Zeyl, R. J., Rotmans, J. P. & Deelder, A. M. Schistosoma mansoni: in vitro and in vivo excretion of CAA and CCA by developing schistosomula and adult worms. *The Journal of parasitology* **82**, 557–64 (1996).
23. Shaw, T. N. *et al.* Tissue-resident macrophages in the intestine are long lived and defined by Tim-4 and CD4 expression. *Journal of Experimental Medicine* **215**, 1507–1518 (2018).
24. Ferrer-Font, L. *et al.* High-dimensional analysis of intestinal immune cells during helminth infection. *eLife* **9**, (2020).

25. Caporaso, J. G. *et al.* Ultra-high-throughput microbial community analysis on the Illumina HiSeq and MiSeq platforms. *The ISME Journal 2012 6:8* **6**, 1621–1624 (2012).
26. Klindworth, A. *et al.* Evaluation of general 16S ribosomal RNA gene PCR primers for classical and next-generation sequencing-based diversity studies. *Nucleic Acids Research* **41**, e1–e1 (2013).
27. Caporaso, J. G. *et al.* QIIME allows analysis of high-throughput community sequencing data. *Nature Methods* **7**, 335–336 (2010).
28. Callahan, B. J. *et al.* DADA2: High-resolution sample inference from Illumina amplicon data. *Nature Methods* **13**, 581–583 (2016).
29. Quast, C. *et al.* The SILVA ribosomal RNA gene database project: improved data processing and web-based tools. *Nucleic Acids Research* **41**, D590 (2013).
30. Zakrzewski, M. *et al.* Calypso: a user-friendly web-server for mining and visualizing microbiome–environment interactions. *Bioinformatics* **33**, 782 (2017).
31. Hepworth, M. R. *et al.* Innate lymphoid cells regulate CD4 + T-cell responses to intestinal commensal bacteria. *Nature* **498**, 113–117 (2013).
32. Costain, A. H., MacDonald, A. S. & Smits, H. H. Schistosome Egg Migration: Mechanisms, Pathogenesis and Host Immune Responses. *Frontiers in immunology* vol. 9 3042 (2018).
33. Cheever, A. W. *et al.* Kinetics Of Egg Production And Egg Excretion By Schistosoma Mansoni And S. Japonicum In Mice Infected With A Single Pair Of Worms. *American Journal Of Tropical Medicine And Hygiene* **50**, 281–295 (1994).
34. Jacobs, W., Deelder, A. & Van Marck, E. Schistosomal granuloma modulation. II. Specific immunogenic carbohydrates can modulate schistosome-egg-antigen-induced hepatic granuloma formation. *Parasitology Research* **85**, 14–18 (1999).
35. Chassaing, B. *et al.* Fecal Lipocalin 2, a Sensitive and Broadly Dynamic Non-Invasive Biomarker for Intestinal Inflammation. *PLoS ONE* **7**, (2012).
36. Grzych, J. M. *et al.* Egg deposition is the major stimulus for the production of Th2 cytokines in murine schistosomiasis mansoni. *Journal of immunology (Baltimore, Md. : 1950)* **146**, 1322–7 (1991).
37. Pearce, E. J., Caspar, P., Grzych, J.-M., Lewis, F. A. & Sher, A. *Downregulation of Thl Cytokine Production Accompanies Induction of Th2 Responses by a Parasitic Helrninth, Schistosoma mansoni*.
38. Orecchioni, M., Ghosheh, Y., Pramod, A. B. & Ley, K. Macrophage polarization: Different gene signatures in M1(Lps+) vs. Classically and M2(LPS-) vs. Alternatively activated macrophages. *Frontiers in Immunology* **10**, 1084 (2019).
39. Kay, G. L. *et al.* Differences in the Faecal Microbiome in Schistosoma haematobium Infected Children vs. Uninfected Children. *PLOS Neglected Tropical Diseases* **9**, e0003861 (2015).
40. Adebayo, A. S. *et al.* The microbiome in urogenital schistosomiasis and induced bladder pathologies. *PLoS neglected tropical diseases* **11**, (2017).
41. Schneeberger, P. H. H. *et al.* Investigations on the interplays between Schistosoma mansoni, praziquantel and the gut microbiome. *Parasites and Vectors* **11**, 1–12 (2018).
42. Ajibola, O. *et al.* Urogenital schistosomiasis is associated with signatures of microbiome dysbiosis in Nigerian adolescents. *Scientific Reports 2019 9:1* **9**, 1–15 (2019).
43. Jenkins, T. P. *et al.* Schistosoma mansoni infection is associated with quantitative and qualitative modifications of the mammalian intestinal microbiota. *Scientific Reports* **8**, 12072 (2018).
44. Visconti, A. *et al.* Interplay between the human gut microbiome and host metabolism. *Nature Communications 2019 10:1* **10**, 1–10 (2019).
45. Webster, H. C., Andrusaite, A. T., Shergold, A. L., Milling, S. W. F. & Perona-Wright, G. Isolation and functional characterisation of lamina propria leukocytes from helminth-infected, murine small intestine. *Journal of Immunological Methods* **477**, 112702 (2020).
46. Mowat, A. M. I., Scott, C. L. & Bain, C. C. Barrier-tissue macrophages: functional adaptation to environmental challenges. *Nature Medicine 2017 23:11* **23**, 1258–1270 (2017).

47. Maizels, R. M. & Mcsorley, H. J. Regulation of the host immune system by helminth parasites. *Journal of Allergy and Clinical Immunology* (2016) doi:10.1016/j.jaci.2016.07.007.
48. Buchanan, R. D., Fine, D. P. & Colley, D. G. Schistosoma mansoni Infection in Mice Depleted of Thymus-Dependent Lymphocytes: II. Pathology and Altered Pathogenesis. *The American Journal of Pathology* **71**, 207 (1973).
49. Fallon, P. G., Richardson, E. J., Smith, P. & Dunne, D. W. Elevated type 1, diminished type 2 cytokines and impaired antibody response are associated with hepatotoxicity and mortalities during Schistosoma mansoni infection of CD4-depleted mice. *European Journal of Immunology* **30**, 470–480 (2000).
50. Brunet, L. R., Finkelman, F. D., Cheever, A. W., Kopf, M. A. & Pearce, E. J. IL-4 protects against TNF-alpha-mediated cachexia and death during acute schistosomiasis. *Journal of immunology (Baltimore, Md. : 1950)* **159**, 777–85 (1997).
51. Herbert, D. R. *et al.* Alternative macrophage activation is essential for survival during schistosomiasis and downmodulates T helper 1 responses and immunopathology. *Immunity* **20**, 623–635 (2004).
52. Onguru, D. *et al.* Human schistosomiasis is associated with endotoxemia and Toll-like receptor 2- and 4-bearing B cells. *The American journal of tropical medicine and hygiene* **84**, 321–4 (2011).
53. Wang, L. *et al.* Methods to determine intestinal permeability and bacterial translocation during liver disease. *Journal of Immunological Methods* **421**, 44–53 (2015).
54. Schoultz, I. & Keita, Å. v. The Intestinal Barrier and Current Techniques for the Assessment of Gut Permeability. *Cells* **9**, (2020).
55. Mowat, A. M. I. To respond or not to respond - A personal perspective of intestinal tolerance. *Nature Reviews Immunology* vol. 18 405–415 (2018).
56. Rapin, A. & Harris, N. L. Helminth–Bacterial Interactions: Cause and Consequence. *Trends in Immunology* vol. 39 724–733 (2018).
57. Harris, N. L. & Loke, P. Recent Advances in Type-2-Cell-Mediated Immunity: Insights from Helminth Infection. *Immunity* vol. 47 1024–1036 (2017).
58. McDole, J. R. *et al.* Goblet cells deliver luminal antigen to CD103 + dendritic cells in the small intestine. *Nature* **483**, 345–349 (2012).
59. McKay, D. M., Shute, A. & Lopes, F. Helminths and intestinal barrier function. *Tissue Barriers* vol. 5 (2017).
60. Robinson, M. W. *et al.* A Family of Helminth Molecules that Modulate Innate Cell Responses via Molecular Mimicry of Host Antimicrobial Peptides. *PLOS Pathogens* **7**, e1002042 (2011).
61. Martin, I., Cabán-Hernández, K., Figueroa-Santiago, O. & Espino, A. M. Fasciola hepatica Fatty Acid Binding Protein Inhibits TLR4 Activation and Suppresses the Inflammatory Cytokines Induced by Lipopolysaccharide In Vitro and In Vivo . *The Journal of Immunology* **194**, 3924–3936 (2015).
62. Taylor, J. J., Krawczyk, C. M., Mohrs, M. & Pearce, E. J. Th2 cell hyporesponsiveness during chronic murine schistosomiasis is cell intrinsic and linked to GRAIL expression. *Journal of Clinical Investigation* **119**, 1019–1028 (2009).
63. Gondorf, F. *et al.* Chronic Filarial Infection Provides Protection against Bacterial Sepsis by Functionally Reprogramming Macrophages. *PLoS Pathogens* **11**, 1–27 (2015).
64. Bessman, N. J. *et al.* Dendritic cell-derived hepcidin sequesters iron from the microbiota to promote mucosal healing. *Science* **368**, 186–189 (2020).
65. McDonald, B. *et al.* Programing of an Intravascular Immune Firewall by the Gut Microbiota Protects against Pathogen Dissemination during Infection. *Cell Host & Microbe* **28**, 660-668.e4 (2020).
66. Smith, K., McCoy, K. D. & Macpherson, A. J. Use of axenic animals in studying the adaptation of mammals to their commensal intestinal microbiota. *Seminars in Immunology* **19**, 59–69 (2007).
67. Mazmanian, S. K., Cui, H. L., Tzianabos, A. O. & Kasper, D. L. An Immunomodulatory Molecule of Symbiotic Bacteria Directs Maturation of the Host Immune System. *Cell* **122**, 107–118 (2005).

68. Atarashi, K. *et al.* Treg induction by a rationally selected mixture of Clostridia strains from the human microbiota. *Nature* **500**, 232–6 (2013).
69. MB, G. *et al.* Intestinal bacterial colonization induces mutualistic regulatory T cell responses. *Immunity* **34**, 794–806 (2011).
70. Ivanov, I. I. *et al.* Induction of intestinal Th17 cells by segmented filamentous bacteria. *Cell* **139**, 485–98 (2009).
71. Prout, M. S., Kyle, R. L., Ronchese, F. & le Gros, G. IL-4 Is a Key Requirement for IL-4- and IL-4/IL-13-Expressing CD4 Th2 Subsets in Lung and Skin. *Frontiers in Immunology* **0**, 1211 (2018).
72. Saluzzo, S. *et al.* First-Breath-Induced Type 2 Pathways Shape the Lung Immune Environment. *Cell Reports* **18**, 1893 (2017).
73. de Kleer, I. M. *et al.* Perinatal Activation of the Interleukin-33 Pathway Promotes Type 2 Immunity in the Developing Lung. *Immunity* **45**, 1285–1298 (2016).
74. Reynolds, L. A. *et al.* Commensal-pathogen interactions in the intestinal tract. *Gut Microbes* **5**, 522–532 (2014).
75. TG, T. *et al.* Identifying species of symbiont bacteria from the human gut that, alone, can induce intestinal Th17 cells in mice. *Proceedings of the National Academy of Sciences of the United States of America* **113**, E8141–E8150 (2016).
76. Hacohen, N. *et al.* Schistosomiasis Th17 Cell Responses in Murine Critical for the Development of Pathogenic CD209a Expression on Dendritic Cells Is. (2021) doi:10.4049/jimmunol.1400121.
77. Shainheit, M. G. *et al.* The pathogenic Th17 cell response to major schistosome egg antigen is sequentially dependent on IL-23 and IL-1β. *Journal of immunology (Baltimore, Md. : 1950)* **187**, 5328–5335 (2011).
78. Floudas, A., Amu, S. & Fallon, P. G. New Insights into IL-10 Dependent and IL-10 Independent Mechanisms of Regulatory B Cell Immune Suppression. *Journal of Clinical Immunology* **36**, 25–33 (2016).
79. Britton, G. J. *et al.* Defined microbiota transplant restores Th17/RORγt+ regulatory T cell balance in mice colonized with inflammatory bowel disease microbiotas. *Proceedings of the National Academy of Sciences* **117**, 21536–21545 (2020).
80. Pandiyan, P. *et al.* Microbiome Dependent Regulation of Tregs and Th17 Cells in Mucosa. *Frontiers in Immunology* **0**, 426 (2019).
81. Ohnmacht, C. *et al.* The microbiota regulates type 2 immunity through RORγt+ T cells. *Science* **349**, 989–993 (2015).
82. Bloom, S. M. *et al.* Commensal Bacteroides Species Induce Colitis in Host-Genotype-Specific Fashion in a Mouse Model of Inflammatory Bowel Disease. *Cell Host & Microbe* **9**, 390–403 (2011).
83. Parker, B. J., Wearsch, P. A., Veloo, A. C. M. & Rodriguez-Palacios, A. The Genus Alistipes: Gut Bacteria With Emerging Implications to Inflammation, Cancer, and Mental Health. *Frontiers in Immunology* **11**, (2020).
84. JL, R. & SK, M. Inducible Foxp3+ regulatory T-cell development by a commensal bacterium of the intestinal microbiota. *Proceedings of the National Academy of Sciences of the United States of America* **107**, 12204–12209 (2010).
85. Ramanan, D. *et al.* Helminth Infection Promotes Colonization Resistance via Type 2 Immunity. *Science (New York, N.Y.)* **352**, 608 (2016).
86. Rausch, S. *et al.* Parasitic nematodes exert antimicrobial activity and benefit from microbiota-driven support for host immune regulation. *Frontiers in Immunology* **9**, 2282 (2018).
87. Reynolds, L. A., Finlay, B. B. & Maizels, R. M. Cohabitation in the Intestine: Interactions among Helminth Parasites, Bacterial Microbiota, and Host Immunity. *The Journal of Immunology* **195**, 4059–4066 (2015).
88. Alam, A. & Neish, A. Role of gut microbiota in intestinal wound healing and barrier function. *Tissue Barriers* **6**, (2018).

89. Ramanan, D. *et al.* Helminth infection promotes colonization resistance via type 2 immunity. *Science* **352**, 608–612 (2016).
90. Hu, Z. *et al.* Small proline-rich protein 2A is a gut bactericidal protein deployed during helminth infection. *Science* **374**, eabe6723 (2021).
91. Grencis, R. K. & Worthington, J. J. Tuft Cells: A New Flavor in Innate Epithelial Immunity. *Trends in Parasitology* vol. 32 583–585 (2016).
92. Harris, T. A. *et al.* Resistin-like Molecule α Provides Vitamin-A-Dependent Antimicrobial Protection in the Skin. *Cell Host & Microbe* **25**, 777-788.e8 (2019).
93. AJ, M. & T, U. Induction of protective IgA by intestinal dendritic cells carrying commensal bacteria. *Science (New York, N.Y.)* **303**, 1662–1665 (2004).
94. Rausch, S. *et al.* Parasitic nematodes exert antimicrobial activity and benefit from microbiota-driven support for host immune regulation. *Frontiers in Immunology* **9**, (2018).
95. Zheng, D., Liwinski, T. & Elinav, E. Interaction between microbiota and immunity in health and disease. *Cell Research 2020 30:6* **30**, 492–506 (2020).
96. Campbell, C. *et al.* Bacterial metabolism of bile acids promotes generation of peripheral regulatory T cells. *Nature 2020 581:7809* **581**, 475–479 (2020).
97. X, S. *et al.* Microbial bile acid metabolites modulate gut RORγ + regulatory T cell homeostasis. *Nature* **577**, 410–415 (2020).
98. Burgess, S. L. *et al.* Gut microbiome communication with bone marrow regulates susceptibility to amebiasis. *The Journal of Clinical Investigation* **130**, 4019 (2020).
99. Grüner, N. & Mattner, J. Bile Acids and Microbiota: Multifaceted and Versatile Regulators of the Liver–Gut Axis. *International Journal of Molecular Sciences* **22**, 1–17 (2021).
100. Grainger, J. R. *et al.* Inflammatory monocytes regulate pathologic responses to commensals during acute gastrointestinal infection. *Nature medicine* **19**, 713 (2013).

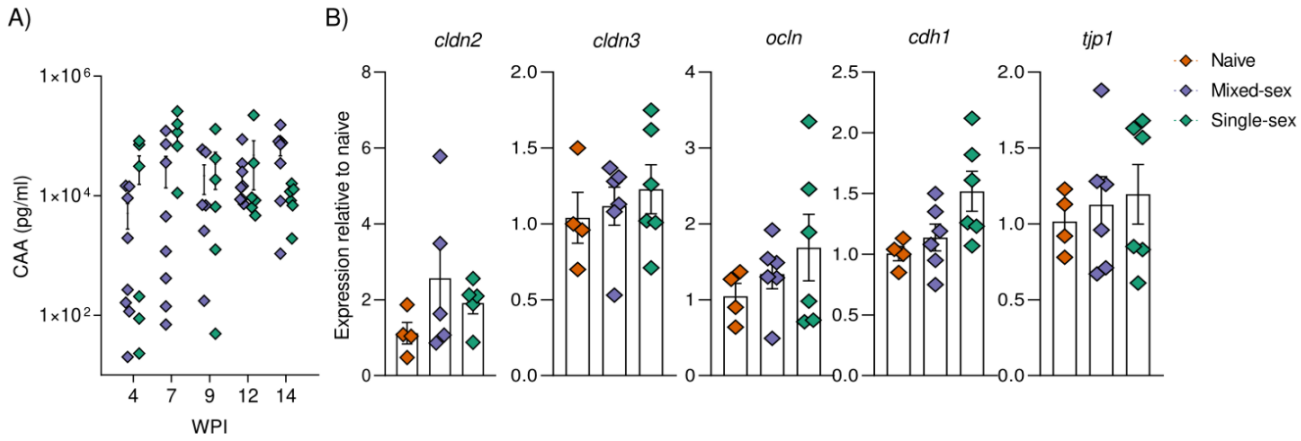

Supplementary Figure 1. Comparable infection loads and expression of tight junction genes in egg producing and non-egg producing infections. (A) Serum levels of the regurgitated worm product Circulating anodic antigen (CAA) in mixed-sex and single-sex infected mice (B) The expression of tight junction associated genes in the colonic tissue of naïve, mixed-sex and single-sex infected mice at week 14 of infection. Data normalized against HK pool (RPLP0, β2m, β-actin and s18) and represented as fold change relative to naïve. Data presented as mean +/- SEM. n=4-8 from one single experiment. Statistical analysis conducted by one-way ANOVA.

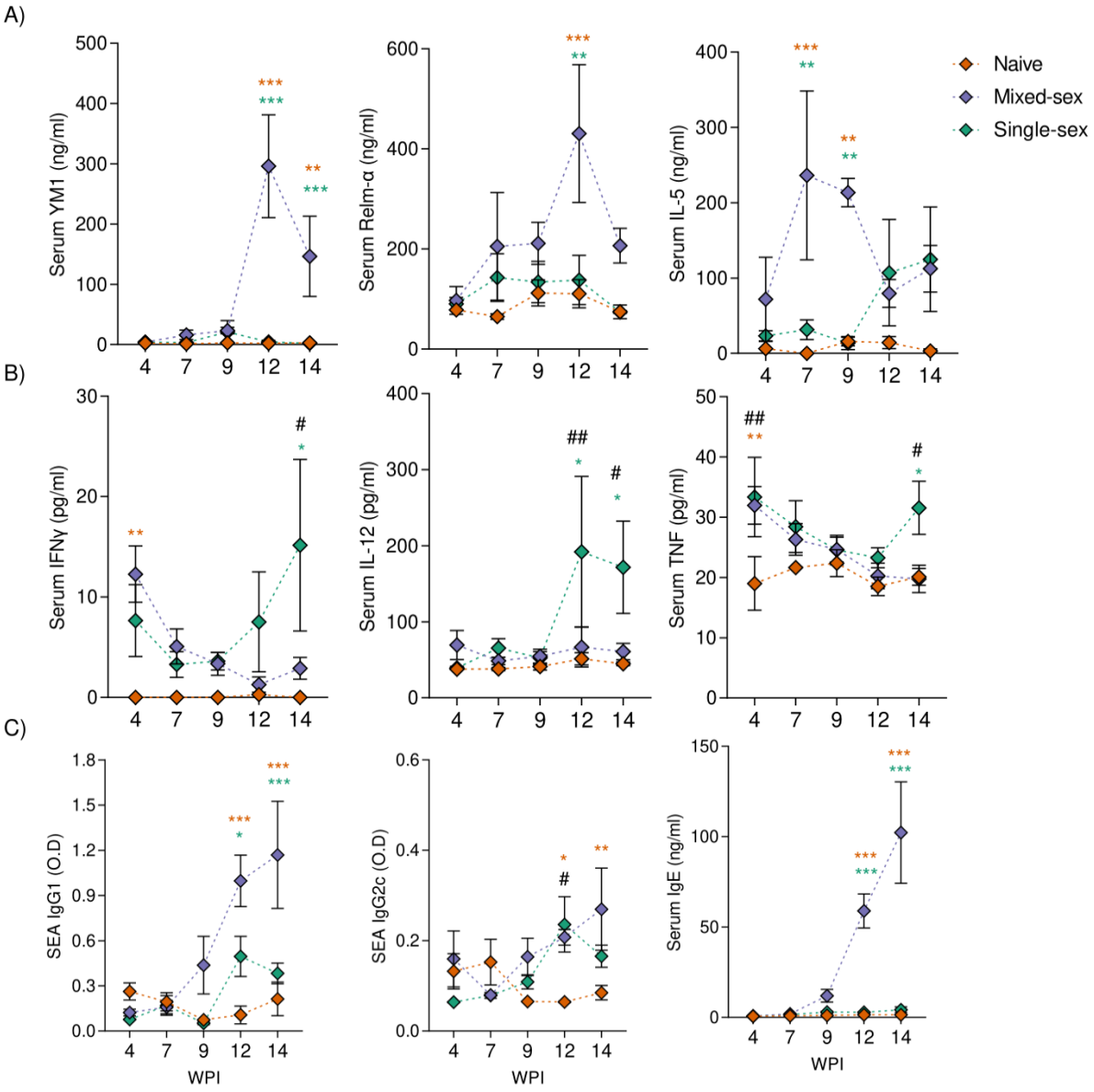

Supplementary Figure 2. Systemic Th2 polarisation in mixed-sex infections only. (A) Serum levels of Th2 associated mediators (Ym1, RELMα) and cytokines (IL-5), (B) Th1 associated cytokines (IFNγ, TNFα and IL-12) and (C) SEA-specific antibodies (IgG1 and IgG2c) and total IgE across the course of infection. Data presented as mean +/- SEM. n=6-8 from a single experiment. Significant differences are indicated by * $p < 0.05$, ** $p < 0.01$, *** $p < 0.001$ and determined by two-way ANOVA. Significant differences between naïve vs mixed-sex infected mice, and single-sex vs mixed-sex infected mice are indicted by orange (*) and green asterisks (*) respectively. Significant differences between naïve and single-sex infected mice are indicated by #.

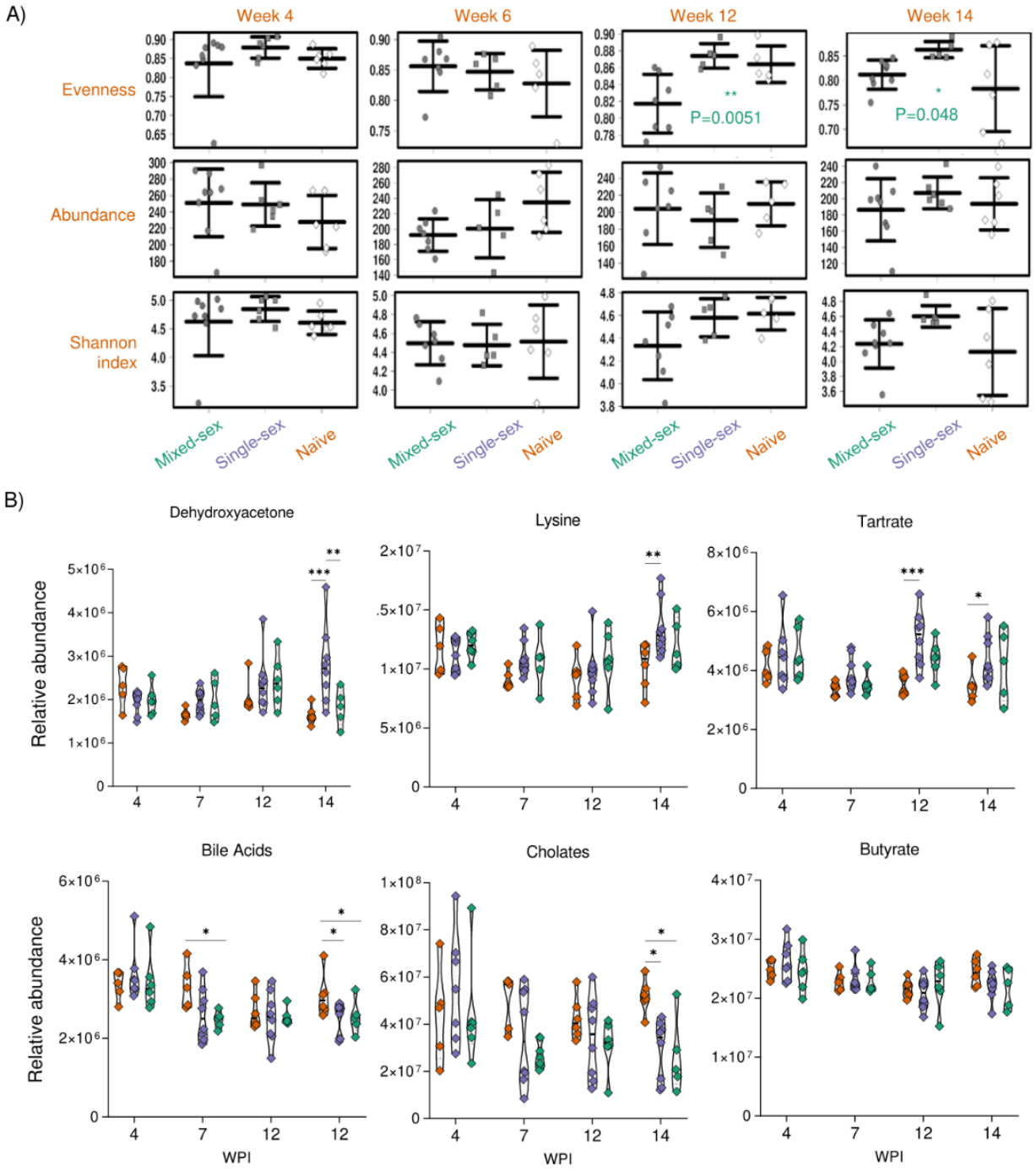

Supplementary figure 3. Schistosome egg transit reduces microbial evenness and the impacts metabolic profile of the small intestine. (A) Differences in microbial alpha diversity in infected and non-infected mice as measured by species evenness, abundance, and Shannon diversity. (B) The relative abundance of small intestinal metabolites was determined by NMR spectroscopy. Data from one single experiment with n=5-7. Significant differences between each group are indicated by * $p < 0.05$, ** $p < 0.01$, *** $p < 0.001$ and calculated by one-way ANOVA (A) or two-way ANOVA (B) followed by Tukey's post doc.

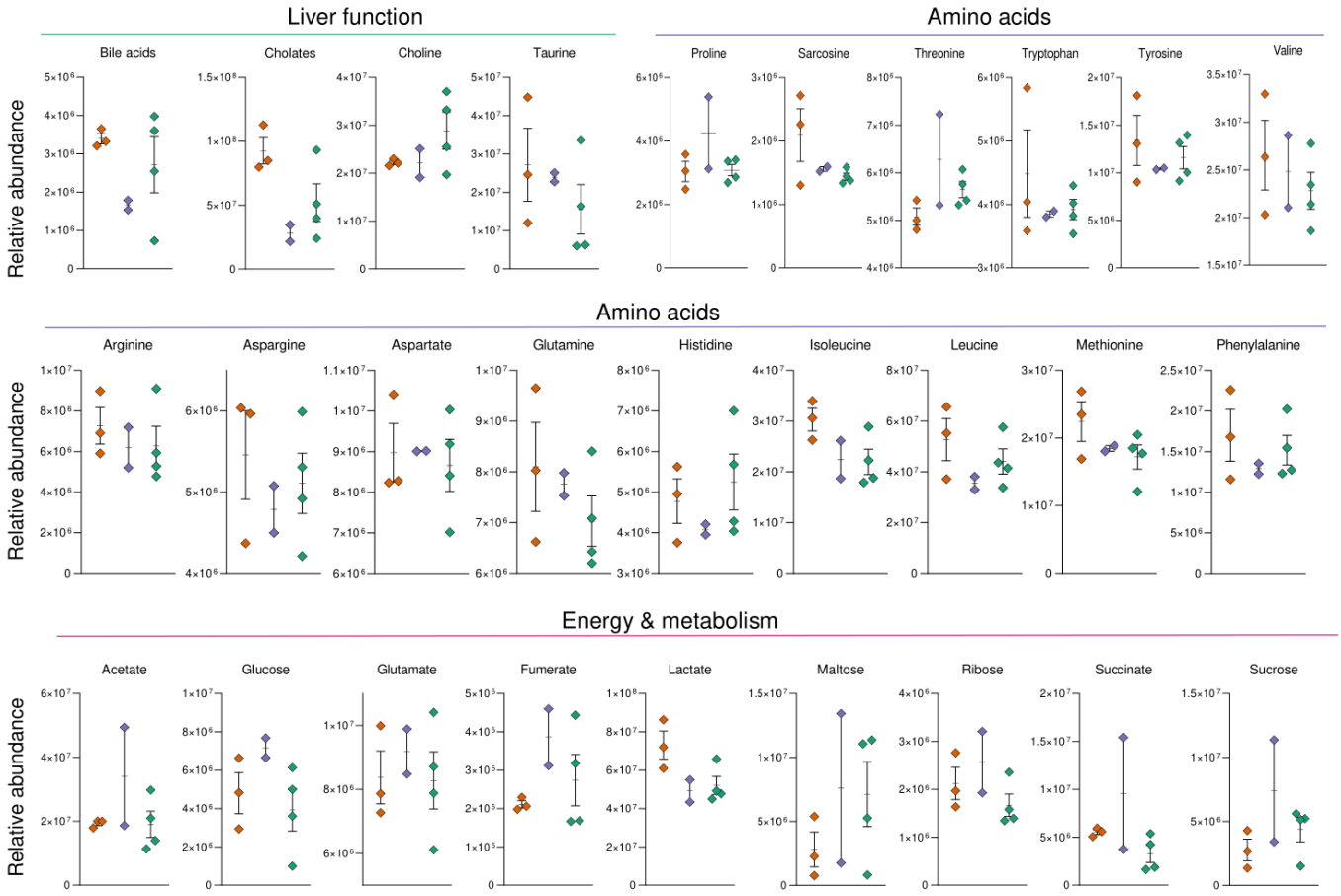

Supplementary Figure 4. Intestinal metabolomics. The abundance of small intestinal metabolites was determined by NMR spectroscopy. Data from one single experiment with n=5-7. Significant differences are indicated by * $p < 0.05$, ** $p < 0.01$, *** $p < 0.001$

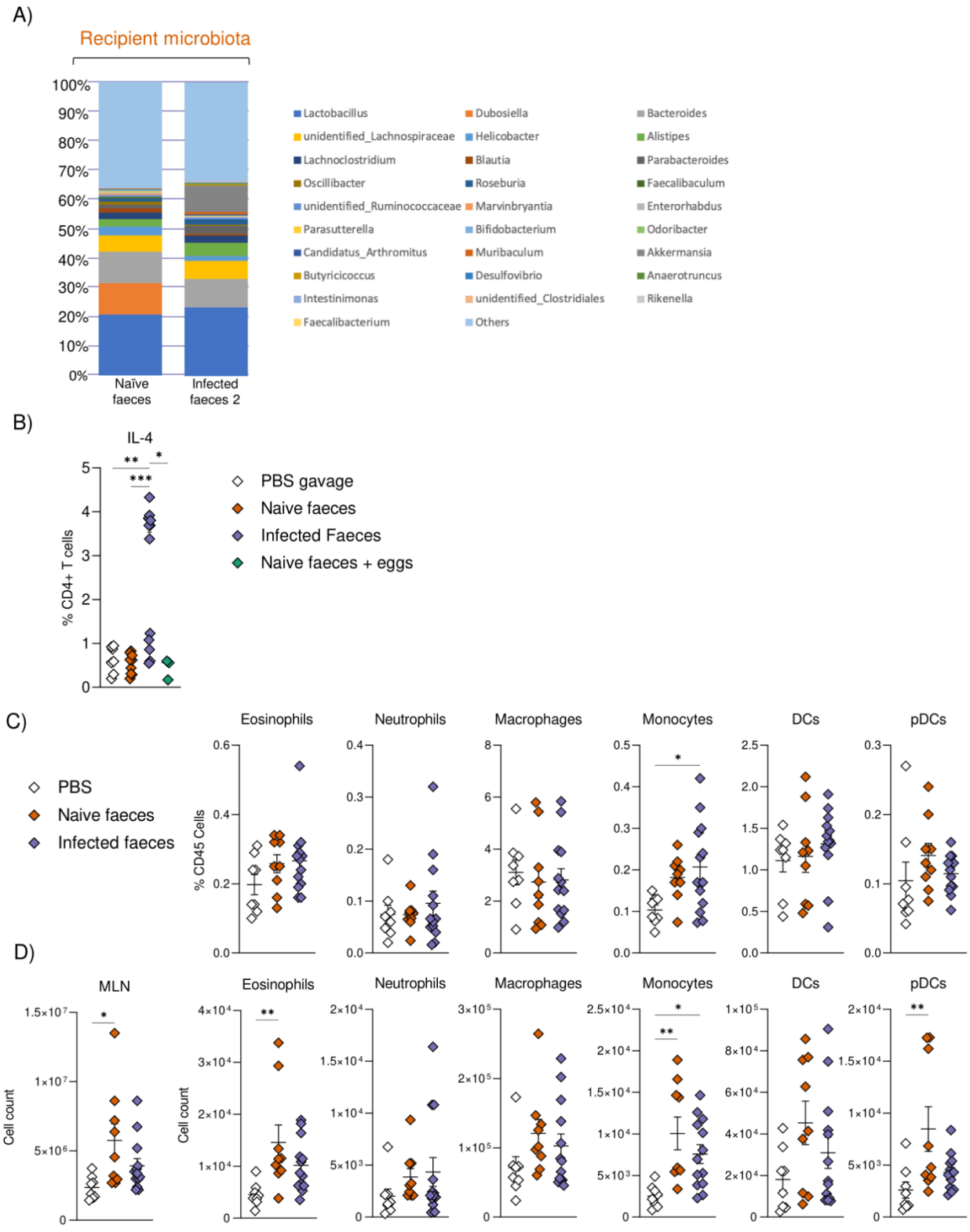

Supplementary Figure 5. Characterisation of faecal transplant microbiotas and immune responses. (A) Bar charts representing the 20 most abundant genera detected in the colonic content of faecal transplant recipients. 16s sequencing was conducted on pooled faecal donor or recipient samples, with 3-4 samples pooled per group. (B) IL-4 secretion in PMA stimulated MLN CD4+ T cells after 2 weeks of faecal recolonisation. To control for the effect of egg-derived antigens, a separate cohort of mice were gavaged with naïve faeces spiked with approx. 1000 S. mansoni eggs. The (C) frequency and (D) absolute numbers of indicated cell types in the MLNs and of GF mice receiving faecal transplant. (B=D) Data presented as mean +/- SEM. Data pooled from two (B) or three pooled experiments (C&D). n=3-13 mice per group. Significant differences were determined by one-way ANOVA followed by Tukey's post hoc test. *p < 0.05, **p < 0.01, ***p < 0.001.